Functionally graded thermoelectric generator and cooler elements

contribution to the new CRC Handbook - submitted version

E. Müller[a], K. Zabrocki[a], C. Goupil[b], G.J. Snyder[c], and W. Seifert[d]

[a] *Institute of Materials Research, German Aerospace Center (DLR), D-51170 Köln, Germany*

[b] *Laboratoire CRISMAT, UMR 6508, Caen, France*

[c] *California Institute of Technology, Pasadena, California 91125, USA*

[d] *Institute of Physics, University Halle-Wittenberg, Germany*

February 2, 2011

Contents

1 Functionally graded thermoelectric generator and cooler elements

1.1 Introduction

Since the discovery of semiconductor thermoelements, there has been much effort to enhance the efficiency of thermoelectric (TE) devices. Along with efforts to increase a material's figure of merit, the use of Functionally Graded Materials (FGM) offers other ways to further improve device performance [7, 10–12, 18, 19, 38, 44, 56, 57, 61, 72, 82, 89–95, 107, 122–124, 126, 127, 154–157, 159, 162, 165, 166, 168, 169, 173, 182, 183, 185]. Graded thermoelectrics are characterized by a macroscopic gradient in their functional properties, caused by spatial variation of the composition (including doping) or microstructure. Also non-continuously graded (i.e. segmented) elements are considered FGM since they lead to the same functional effect.

Although a TE gradient means a related spatial variation of all TE material properties, the strongest effect is generally linked to the variation of the Seebeck coefficient which is the primary material parameter of TE coupling between thermal and electrical energy transport. This is because a gradient in the Seebeck coefficient is linked to an additional, local heat release or absorption whereas a resistivity gradient will merely gradually shift the location of Joule heat release along the element. A gradient in the thermal conductivity will just cause an asymmetry in the outflow of the internally released heat to the hot and cold terminals and may thus deform the temperature profile along the element. It will tend to concentrate the temperature gradient at regions with low thermal conductivity.

Essentially, the functional effect of TE FGM is already observed in a homogeneous TE element with real, temperature dependent, material properties.

Due to the temperature-bound or explicitly position-dependent Seebeck coefficient, Peltier heat is absorbed or released inside the material. In a homogeneous but temperature-dependent material this is known as Thomson effect. In case of an explicit Seebeck gradient, it is also referred to as distributed Peltier effect or extrinsic Thomson effect (ETE) [13, 14, 28, 82, 93]. Simulations and modeling of TE devices and materials is an important part to get guidelines how to improve them for real life usage, see e.g. [34, 48, 53, 55, 78, 79, 105, 121, 129, 135, 146, 152]. The central target of theoretical TE FGM studies is to elaborate recipes for optimal gradients in the TE material properties which ensure optimum operation of a TE device [18, 19, 107]. Ideally, it would be best to have a local criterion for optimizing global performance; currently local criteria are known for the efficiency of a thermogenerator (TEG) and the coefficient of performance of a Peltier cooler (TEC) [159, 168]. However, global optimization requires constraints for the allowed range of temperature dependent materials properties in the con-

sidered materials. In order to prevent that global performance diverges in the optimization process, limits of the material properties have to be fed into the process, be these upper limits for the Seebeck coefficient and the electrical conductivity and a lower limit for the thermal conductivity, or averages of the TE properties (resp. the figure of merit), of the power factor, or of the efficiency. The optimization strategy we are speaking about here is an optimization strategy due to the material itself. Of course there is the possibility of optimizing other design parameters like the length of an element, its cross-sectional area or the ratio of both [29, 84, 111, 114, 163, 175, 180]. Another aspect would be to include contact resistances into the considerations [8, 37, 110, 112, 115, 117, 145, 146], but this is beyond the scope of this work. Clearly distinguishing from design optimization of real TE devices we will consider here an "ideal" thermogenerator or Peltier device where no thermal losses due to radiation or thermal bypasses, no thermal or electric contact resistance, and only one-dimensional flow is assumed, i.e. electrical current and heat flux are parallel, see also [37]. Every non-parallel arrangement without a magnetic field, where you have an arbitrary angle between the temperature gradient and the electrical current leads to a reduction of the performance which is deduced from a generalized figure of merit shown by Gryaznov and co-workers [64]. For the sake of simplification, a single but representative (segmented or continuously graded) TE generator or cooler element (p-type or n-type, of element length L and constant cross-sectional area $A_{\rm c}$) is often considered as part of a TE device or as a single-element device.[1] Doing this, optimization strategies are based on fixed parameters L and fixed boundary temperatures $T_{\rm a}$ and $T_{\rm s}$ within the framework of a unified 1D model for both TEG and TEC (see Fig. 1.1 and [156]), where $T_{\rm a}$ is the temperature at the heat absorbing side (hot side for TEG, but cold side for TEC), and $T_{\rm s}$ denotes the heat sink temperature which is in many cases fixed not far from the room temperature. The total heat flux and its components in Fig. 1.1 are indicated by the symbols $\mathbf{q} = -\kappa\,\nabla T + \alpha\,T\,\mathbf{j} =: \mathbf{q}_\kappa + \mathbf{q}_\pi$ with Fourier and Peltier heat fluxes $\mathbf{q}_\kappa$ and $\mathbf{q}_\pi$, respectively (see also [157]).[2] Note that all flows are counted positive according to right-headed arrows, thus the magnitude of the flow vectors with left-headed arrows will adopt negative numerical values in the 1D formulae.

---

[1]In a 1D approach the segmentation or grading is clearly in the same direction as the electrical current and the heat flux are. In a quasi-1D or in a multidimensional approach you have to take care of the direction of the electrical current and the heat flow in comparison to the grading direction, see [89–93].

[2]One has to take care of the terms and the notation used. Normally, Q denotes the **heat** in units of 1 J, whereas with $\dot{Q} = \frac{\partial Q}{\partial t}$ the **heat transfer rate, heat flow** or **thermal power** in units of 1 W is meant. For the sake of simplicity the dot is sometimes omitted, as we do here, too. The **heat flux** is often used which is the heat transfer rate per cross-sectional area $q = \frac{1}{A_{\rm c}}\dot{Q} = \frac{1}{A_{\rm c}}\frac{\partial Q}{\partial t}$ in units of 1 W/m².
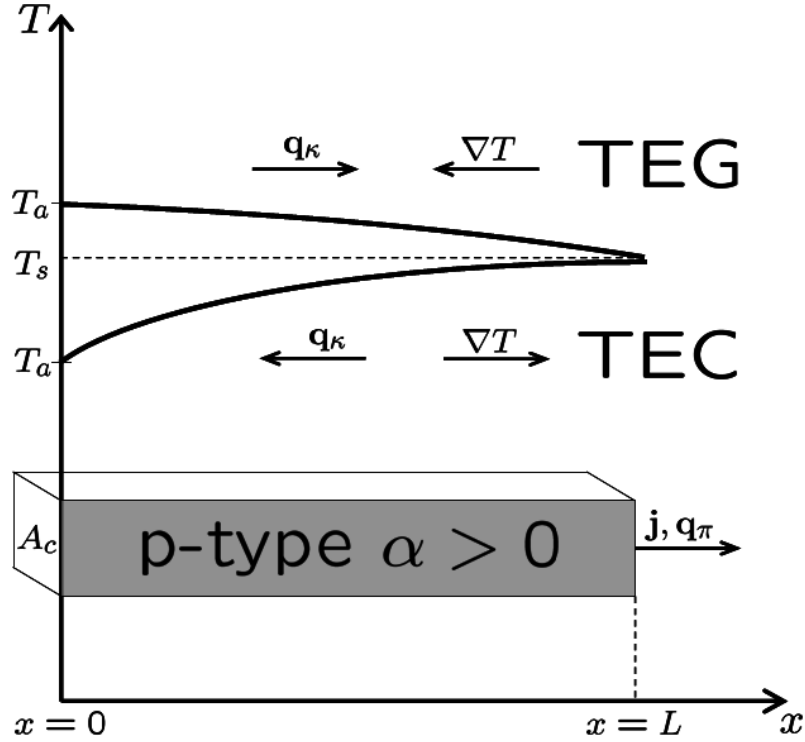
Figure 1.1: Unified 1D model of a thermoelectric element (single p-type pellet of length L, constant cross-sectional area A_c): lower temperature profile: Cooling operation (= TEC case with $T_a < T_s$); upper temperature profile: Thermoelectric generator (= TEG case with $T_a > T_s$). Smaller bowing of the temperature profile in TEG case shall symbolize the relatively lower current in efficient operation, compared to the TEC. Note that $T(x)$ will peak in the interior of the TE element at current values only above the optimum current according to maximum efficiency and maximum coefficient of performance, respectively. This can be shown for the CPM case analytically, see footnote 7.

The different arrow orientations just shall give an idea on the physical flow directions.

All calculations done here are referring to a planar arrangement of prismatic-shaped elements. Other shapes of elements need more detailed consideration, like e. g. circular shape [97–99, 111, 113, 140], where the formulae for the power output may change while the efficiency remains independent of the shape.

On a macroscopic scale, the framework of non-equilibrium thermodynamics with Onsager's approach of a linear response theory is used [130–132]. Under isotropic conditions, the constitutive relations are

$$\mathbf{j} = \sigma\,\mathbf{E} - \sigma\,\alpha\,\nabla T\ , \qquad \mathbf{q} = \alpha\,T\,\mathbf{j} - \kappa\,\nabla T\ , \tag{1.1}$$

with the electric field vector $\mathbf{E}$, electrical current density $\mathbf{j}$, temperature T, total heat flux $\mathbf{q}$, Del operator (or nabla operator) ∇, and the material properties isothermal electrical

conductivity σ, resistivity $\rho = 1/\sigma$, thermal conductivity κ under zero current and Seebeck coefficient α. Note that in general all the material properties are tensors and need then a generalized description, especially if an additional magnetic field is present [4–6, 9, 26, 27, 64, 70, 150].

Assuming steady-state conditions, the governing equations result from the principles of conservation of charge and energy

$$\nabla \cdot \mathbf{j} = 0 \;, \qquad \nabla \cdot \mathbf{q} = \mathbf{j} \cdot \mathbf{E} \;, \tag{1.2}$$

leading to the thermal energy balance in vector notation

$$\nabla \cdot (-\kappa \; \nabla T) = \frac{\mathbf{j}^2}{\sigma} - T \, \mathbf{j} \cdot \nabla \alpha \;. \tag{1.3}$$

Thereby, the electrical current density $\mathbf{j}$ is a constant due to the 1D approach. It fulfills the continuity constraint in one dimension and satisfies $\nabla \cdot \mathbf{j} = \frac{\partial}{\partial x} j_x = 0 \Rightarrow j_x =$ const. Eq. (1.3) makes clear that Joule's heat and a gradient in the Seebeck coefficient appear as sources of the thermal heat flux. Note that the Peltier-Thomson term $T \, \mathbf{j} \cdot \nabla \alpha$ contains both the usual Thomson contribution (temperature gradient effect with a temperature dependent Seebeck coefficient) and the Peltier contribution (spatial gradient effect, see also [28]): $T \, \mathbf{j} \cdot \nabla \alpha = \mathbf{j} \cdot (\nabla \Pi - \alpha \nabla T)$ with the Peltier coefficient $\Pi = \alpha \, T$ and $\nabla \Pi = \frac{d\Pi}{dT} \nabla T = (\alpha + T \frac{d\alpha}{dT}) \nabla T$.

For detailed commentary on Onsager's approach see the original articles [130–132]. Especially for application in thermoelectrics Domenicali denoted the approach of the *Onsager-de Groot-Callen* theory as a kind of "field theory" of the thermodynamics of irreversible phenomena in terms of vector functions which are dependent on temperature and position in general, see [31–33, 40–45, 52, 108, 130–132, 134, 136, 142] for details.

In the next Section 1.2 the fundamentals of a thermodynamic optimization are introduced together with the definition of the entropy production, the thermoelectric potential and local reduced efficiencies. After that, alternative optimization variants will be discussed in section 1.3, especially the differences taking into account local and/or temperature dependence of the properties. In section 1.4 starting with the Constant Properties Model (CPM) the known averaging procedures are introduced and valued. Section 1.5 is dedicated to highlight a "model-free setup" based on spatial material profiles, where you find a summary on numerical and analytical solutions of the thermal energy balance equation. The relation

between the compatibility approach and optimum material grading is shown in Section 1.6. In the final two Sections 1.7 and 1.8 a short summary and an outlook to related problems are given.

1.2 Thermodynamic optimization and minimum of entropy production

Thermoelectric effects are caused by coupling between heat and charge transport of the electronic "fluid" [32]. For a deeper understanding of TE processes as processes out of thermodynamic equilibrium we highly recommend the article by C.B. Vining [179]. The description on a mesoscopic level is based on a stationary picture where all the thermodynamic potential functions are clearly defined, though the system itself produces dissipation. Since the inherent relaxation times are much smaller than the time scale of the varying potentials, this description is also a definition of a quasi-static process. As a consequence, the classical quasi-static relation $dS = \delta Q/T$ between the heat and the entropy variation is fully valid and can be expressed in terms of the entropy and heat current densities through $\mathbf{j}_S = \mathbf{q}/T$. In close connection with the general linear response theory this leads to the well-known coupled set of equations for heat flux and particle flux [31, 32]

$$
\begin{bmatrix} \mathbf{j}_N \\ \mathbf{q} \end{bmatrix} = \begin{bmatrix} L_{11} & L_{12} \\ L_{21} & L_{22} \end{bmatrix} \begin{bmatrix} -\frac{1}{T}\nabla\mu \\ \nabla(\frac{1}{T}) \end{bmatrix},
\tag{1.4}
$$

where μ is the Gibbs electrochemical potential (as sum of the chemical potential and the electrical potential), $\mathbf{j}_N$ the carriers flux, and $\mathbf{q}$ the heat flux. $\frac{1}{T}\nabla\mu$ and $\nabla(\frac{1}{T})$ are the forces corresponding to the electrochemical and thermal potentials, respectively. As a dissipative system, the system's evolution is driven by a minimal production of entropy where each fluctuation of any thermodynamic potential is subjected to a restoring force to equilibrium [142]. This concept had already been used by Clingman [35, 36] who set out to use minimum entropy production to derive optimum device performance, for details we also refer to [63]. The symmetry of the off-diagonal terms $L_{ij} = L_{ji}$, as generally expected from Onsager's reciprocal relation, is equivalent to a minimal entropy production of the system under out-of-equilibrium conditions [142]. The kinetic coefficients L_{ij} can easily be expressed using material parameters leading to $L_{11} = \frac{T}{e^2}\sigma$, $L_{12} = -\frac{T^2}{e^2}\sigma S_J$, $L_{22} = \frac{T^3}{e^2}\sigma S_J^2 + T^2\kappa$, where

$S_J = \alpha e$ is the so-called entropy per carrier, see e. g. [32, 43–45]. Using the local expansion $\nabla \frac{1}{T} = -\frac{1}{T^2} \nabla T$ and $\mathbf{E} = -\frac{\nabla \mu}{e}$, Eq. (1.1) is reproduced [179].

For decades, the figure of merit $z = \alpha^2 \sigma / \kappa$ has provided a measure of the quality of a thermoelectric material, for details see Section 1.4.2 and 1.4.3. A general rule is, that if a material is good (high $z\,T$) then it is good in both TEG and cooler applications.

1.2.1 Volumic entropy production

Since the entropy flux is $\mathbf{j}_S = \mathbf{q}/T$, it follows that the volumic entropy production ν_S is directly given by $\nabla \cdot \mathbf{j}_S = \nabla \cdot (\mathbf{q}/T)$ which gives with Eqs. (1.1) and (1.2)

$$\nu_S = \nabla \cdot \mathbf{j}_S = \mathbf{q} \cdot \nabla \left(\frac{1}{T} \right) + \frac{\mathbf{j} \cdot \mathbf{E}}{T} = -\kappa \nabla T \cdot \nabla \left(\frac{1}{T} \right) + \frac{1}{T} \frac{j^2}{\sigma} \,, \tag{1.5}$$

where we identify the Joule and non-isothermal conduction contributions to the entropy. This expression can be rewritten with $\mathbf{E} = -\frac{\nabla \mu}{e}$ in the form $\nabla \cdot \mathbf{j}_S = \mathbf{q} \cdot \nabla \left(\frac{1}{T} \right) + \left(\frac{\nabla \mu}{eT} \right) \cdot (-\mathbf{j})$. One can notice that the volumic entropy production is simply obtained from the summation of the force-flux products [31, 32].

1.2.2 Thermoelectric potential

Introducing the relative current density u defined[3] as the ratio of electrical current density $\mathbf{j}$ to the Fourier fraction of the heat flux $\mathbf{q}_\kappa$ with respect to the flow direction of $\mathbf{j} = j\,\mathbf{n}$

$$u = -\frac{\mathbf{j} \cdot \mathbf{n}}{\kappa \, \nabla T \cdot \mathbf{n}} \quad \text{resp.} \quad 1/u = -\frac{\kappa \, \nabla T \cdot \mathbf{j}}{\mathbf{j} \cdot \mathbf{j}} \,. \tag{1.6}$$

Note again that the fluxes are in parallel and Eq. (1.6) is just the ratio of the projections onto the direction of the fluxes. Alternatively you can choose your coordinate system such that the flux direction is similar to one axis. Heat and particle fluxes can be combined giving

$$\mathbf{q} = \Phi \mathbf{j} = \left[\alpha T + \frac{1}{u} \right] \mathbf{j} \,, \tag{1.7}$$

---

[3]The gradient ∇T is a vector; avoid therefore the definition $u = -\frac{j}{\kappa \nabla T}$, instead use the 1D variants $u(x) = -\frac{j}{\kappa T'(x)}$ resp. $u(T) = -\frac{j}{\kappa} x'(T)$. For a more general definition of u see footnote 13.

where Φ is the thermoelectric potential as defined by Snyder [100,101,165,166,168,169,176].

These expressions allow a simple derivation of the volumic heat production ν_q from

$$\nu_q = \nabla \cdot \mathbf{q} = \mathbf{j} \cdot \nabla \Phi = \mathbf{j} \cdot \nabla \left[\alpha\, T + \frac{1}{u} \right] \; . \tag{1.8}$$

Then we directly obtain the heat production density from the degradation of the potential Φ. Since the entropy flux is $\mathbf{j}_S = \Phi\, \mathbf{j}/T$, the volumic entropy production becomes

$$\nu_S = \nabla \cdot \mathbf{j}_S = \mathbf{j} \cdot \nabla \left(\frac{\Phi}{T} \right) \quad \text{or} \quad \nu_S = \frac{\nu_q}{T} + \mathbf{q} \cdot \nabla \left(\frac{1}{T} \right) \; . \tag{1.9}$$

This is in agreement with the classical Onsager formulation where the volumic entropy production is given by the summation of the flux-force product. Then, for a given material, the Φ potential gives a direct measure of the total volumic heat and entropy production by the respective degradation of $\nabla \Phi$ and $\nabla \left(\frac{\Phi}{T} \right)$. From these latter expressions we see that Φ is the correct thermodynamic potential for characterizing thermoelectric processes and systems, respectively.

1.2.3 Local reduced efficiency of TEG and TEC

Following [166], Section 9.2.2. and [156] we can conclude that the local performance of an infinitesimal segment of a TE element of length dx with $dT = T'(x)\, dx$ can be defined as

$$\eta_{\mathrm{loc}} = \frac{dT}{T}\, \eta_{\mathrm{r}} \quad \text{and} \quad \varphi_{\mathrm{loc}} = \frac{T}{dT}\, \varphi_{\mathrm{r}} \; , \tag{1.10}$$

where dT/T is the infinitesimal Carnot cycle factor for TEG and T/dT the one for TEC. As the Carnot process is a reversible one, the reduced "efficiencies"[4] η_{r} and φ_{r} play the role of an "irreversibility factor" which at least measures the distance to reversibility for both TEG and TEC due to a non-perfect TE engine. Such considerations were published first by E. Altenkirch [2,3].

The reduced efficiency of a thermogenerator η_{r} is defined as the ratio of the products of conjugated forces and fluxes [168] where we have to pay attention to the fact that the electrical power production in a volume dV is given by the production density $\pi_{el} = \mathbf{j} \cdot \mathbf{E}$, also denoted as differential electrical power. Note that the net differential power output is

---

[4]In [156] and [159] reduced efficiencies $\eta_{\mathrm{r}}^{(g)} \equiv \eta_{\mathrm{r}}$, $\eta_{\mathrm{r}}^{(c)} \equiv \varphi_{\mathrm{r}}$ are introduced for both TEG and TEC, resp.

given by $-\pi_{el}$, see the definition of efficiency in Section 1.3 and [122,153,158]. From Eq. (1.5), we find $\mathbf{j} \cdot \mathbf{E} - T\nu_S = \frac{1}{T}\mathbf{q} \cdot \nabla T = \mathbf{j}_S \cdot \nabla T$, and with $\mathbf{j} \cdot \mathbf{E} = \nabla \cdot \mathbf{q} = \mathbf{j} \cdot \nabla \Phi$ and $\mathbf{j}_S = \Phi \mathbf{j}/T$ we finally get

$$\eta_{\mathrm{r}} = \frac{\mathbf{j} \cdot \mathbf{E}}{\mathbf{j}_S \cdot \nabla T} = \frac{-\pi_{\mathrm{el}}}{-\pi_{\mathrm{el}} - T\nu_S} = \frac{1}{1 + \frac{T\nu_S}{\pi_{\mathrm{el}}}} \quad \implies \quad \eta_{\mathrm{r}} = \frac{T}{\Phi} \frac{\nabla \Phi \cdot \mathbf{j}}{\nabla T \cdot \mathbf{j}} \, , \tag{1.11}$$

which coincides with Clingman's result [35] and corresponds to the reduced variation of the thermoelectric potential $\frac{\nabla \Phi}{\Phi}$ when changing the other potential $\frac{\nabla T}{T}$ which is coherent with a general definition of the efficiency of an out-of-equilibrium thermodynamic process of coupled fluctuating parameters. The reduced efficiency expression can be rewritten from u and Φ expressions, i.e. with $u = \frac{1}{\phi - T\alpha}$ and $\frac{\nabla \Phi \cdot \mathbf{j}}{\nabla T \cdot \mathbf{j}} = \alpha(1 - \frac{\alpha}{z}u)$ resp. $u = -\frac{z}{\alpha^2}\frac{\nabla \Phi \cdot \mathbf{j}}{\nabla T \cdot \mathbf{j}} + \frac{z}{\alpha}$ [166, 168]. The result is for TEG

$$\eta_{\mathrm{r}} = \frac{1 - \frac{u\alpha}{z}}{1 + \frac{1}{uT\alpha}} \qquad = \frac{\frac{u\alpha}{z}\left(1 - \frac{u\alpha}{z}\right)}{\left(\frac{u\alpha}{z} + \frac{1}{zT}\right)} \tag{1.12a}$$

or

$$\eta_{\mathrm{r}} = \frac{1 - \frac{\alpha}{z(\Phi - T\alpha)}}{1 + \frac{z(\Phi - T\alpha)}{zT\alpha}} = \frac{\alpha T}{\Phi}\left(1 - \frac{1}{zT\left(\frac{\Phi}{\alpha T} - 1\right)}\right). \tag{1.12b}$$

An analogous approach can be found for the reduced coefficient of performance of a TEC, φ_{r}. As a consequence of the underlying TE effects (which are inverse to each other, and alike are the definitions of the global performance parameters, efficiency η and coefficient of performance φ)[5], the reduced coefficient of performance φ_{r} is inversely defined

$$\varphi_{\mathrm{r}} = \frac{\mathbf{j}_S \cdot \nabla T}{\mathbf{j} \cdot \mathbf{E}} = \frac{\Phi}{T} \frac{\nabla T \cdot \mathbf{j}}{\nabla \Phi \cdot \mathbf{j}} \, . \tag{1.13}$$

For a direct comparison of TEG and TEC we recommend a unified 1D model for both generator and cooler single elements [156]. Note that $u(T)$ differs formally only by sign if TEG and TEC are operated under reversed boundary temperatures, but otherwise in the same working conditions. For this case of directly comparing TEG and TEC we find formally $\varphi_{\mathrm{r}} = 1/\eta_{\mathrm{r}}$, and the reduced efficiencies present a maximum for $u = s$; where s is the compatibility factor [168] $u_{\mathrm{opt}} = s^{(\mathrm{g})} = \frac{\sqrt{1+zT}-1}{\alpha T}$ of a TEG, but $u_{\mathrm{opt}} = s^{(\mathrm{c})} = \frac{-\sqrt{1+zT}-1}{\alpha T}$

---

[5]We follow Sherman's notation here and use φ instead of *C.O.P.* in TEC formulae.

of a TEC.

The reduced efficiency and local coefficient of performance are defined as functions of u in their ranges of typical use ($0 \leq u \leq 2\,s^{(g)}$ for TEG and $2\,s^{(c)} \leq u \leq 0$ for TEC). In the special situation of maximum local TEG efficiency ($u = s^{(g)} > 0$) and maximum local TEC coefficient of performance ($u = s^{(c)} < 0$) the two values are equivalent $\eta_{\mathrm{r,opt}} = \varphi_{\mathrm{r,opt}} = \frac{\sqrt{1+zT}-1}{\sqrt{1+zT}+1}$, as η_{r} and φ_{r} are local irreversibility factors. This again shows that $z\,T$ is a thermodynamic materials quantity determining the maximum irreversibility factor that is the same for both interrelated thermoelectric effects, Seebeck and Peltier.

The equivalent optimal TE potential is given by

$$\Phi_{\mathrm{opt}}^{(g/c)} = \alpha T + \frac{1}{s^{(g/c)}} = \alpha T \left[\frac{\sqrt{1+zT}}{\sqrt{1+zT}\mp 1}\right] \ , \tag{1.14}$$

where the minus sign applies for TEG, but the plus sign for TEC. Furthermore we find

$$\eta_{\mathrm{r,opt}} = \left(2\frac{\Phi_{\mathrm{opt}}^{(g)}}{\alpha T} - 1\right)^{-1} \quad \text{and} \quad \varphi_{\mathrm{r,opt}} = 2\frac{\Phi_{\mathrm{opt}}^{(c)}}{\alpha T} - 1 \ .$$

The total efficiency η and the total coefficient of performance φ, resp., of a finite generator and a cooler element, resp., are obtained by summing up local contributions based on the reduced efficiency all over the thermoelectric element in an integral sense, see Eqs. (1.31a) and (1.31b). The particular case of maximum performance of an infinitely staged[6] TEG and TEC has been investigated by Sherman and co-workers [160, 161], see Section 1.6.1.

1.2.4 Thermodynamic optimization

For each TE device is known that the current has to be adjusted to an optimal value to reach maximum efficiency or coefficient of performance, resp. The thermodynamic background is explained here. The local treatment leads to an additional requirement concerning TE element design. In Fig. 1.2 we compare the reduced efficiency η_{r} of a TEG for varied values of the dimensionless figure of merit $z\,T$ with the optimal reduced efficiency $\eta_{\mathrm{r,opt}}$ (see also [62]). One can notice that, for a given element, the maximal efficiency can be obtained if the electrochemical potential and the temperature are biased in order to reach $\Phi = \Phi_{\mathrm{opt}}$ all over the system. This "thermodynamic biasing" shows the importance of the working conditions

---

[6]The device (or TE element) is broken up into an infinite number of stages. Note that the terms "perfectly infinitely staged element" and "self-compatible element" as introduced below can be used synonymously.
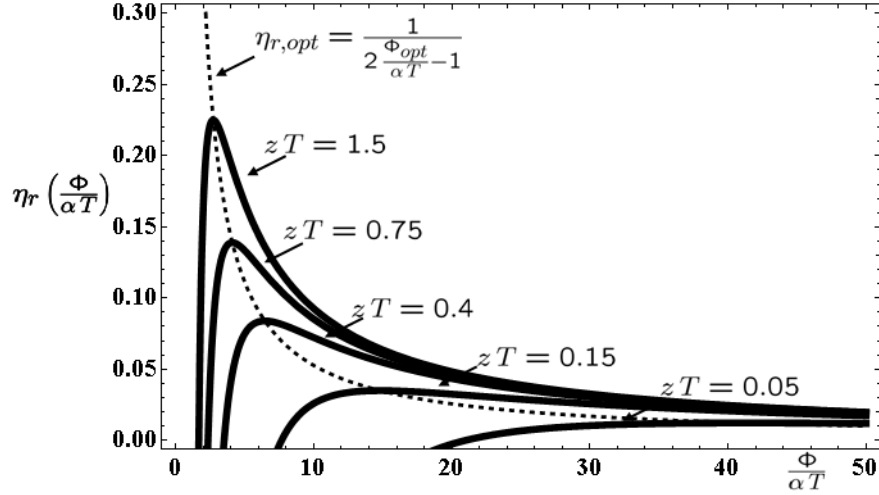
Figure 1.2: Reduced efficiency (irreversibility factor) for TEG as a function of the thermo-electric potential (in units of αT) $\Phi/(\alpha T)$.

of the thermoelectric engine, even at the local scale. As a consequence from Eq. (1.14), FGM must be optimized from the material's point of view, leading to a $zT(T)$ as large as possible, but also from the working conditions point of view. This means in particular that the temperature distribution has to be adjusted to optimum shape. Otherwise the reduced efficiency of each cell (or segment) of a FGM will never reach its maximal attainable value simultaneously.

To sum up, we can draw three conclusions:

1. Simply adjusting maximum zT in each segment of graded TE elements is not sufficient to maximize TE device performance because the operation conditions at each position in the element cannot be adjusted independently from each other but are interrelated by the global condition of a common electrical current crossing each segment of the element.

2. Optimizing the temperature dependence of the material, i. e. $\alpha(T)$, $\sigma(T)$, $\kappa(T)$, is applicable to achieve the maximum local efficiency expected from the zT in each segment of a chemically homogeneous element simultaneously. The compatibility approach is sufficient to achieve this, as will be described below.

3. FGM have to be optimized from a thermodynamic point of view. This should include consideration of the temperature and temperature gradient as will be demonstrated in the next section. Suitable adjustment of $\alpha(x)$, $\sigma(x)$, $\kappa(x)$ implies suitable shaping of the temperature profile.

1.3 Material profiles and performance parameters in the 1D steady state

The reduced "efficiencies" in our one-dimensional approach are given by

$$\eta_{\mathrm{r}}(x) = \frac{1}{\varphi_{\mathrm{r}}(x)} = \frac{\Phi'(x)/\Phi(x)}{T'(x)/T(x)} \quad \text{with} \quad \Phi(x) = \alpha(x)\,T(x) + \frac{1}{u(x)} \ . \tag{1.15}$$

Eq. (1.15) makes clear that the compatibility approach together with additional thermodynamic arguments opens up new opportunities for optimizing the material profiles, see also [63] and Section 1.6.2.

However, before proceeding in this way, we should consider again the TE material properties α, σ and κ which are in general temperature and position dependent quantities and measurable under certain constraints. Here we want to concentrate on decoupled dependencies, i.e. either a temperature **or** spatial dependence of the material coefficients, to gain analytical results for the performance parameters of a TE element. A numerical investigation of a coupled material's local as well as temperature dependence is given by Kaliazin and co-workers [82].

Given the material properties as a function of temperature, Eq. (1.3) reduces in the 1D steady state to

$$\kappa(T)\,\frac{\partial^2 T}{\partial x^2} + \frac{d\kappa}{dT}\,\left(\frac{\partial T}{\partial x}\right)^2 - j\,T\,\frac{d\alpha}{dT}\,\frac{\partial T}{\partial x} = -\,\frac{j^2}{\sigma(T)} \ , \tag{1.16}$$

where a constant current density j is supposed to flow in x-direction (see e.g. [154]).

It is important to note that if there is a "one-to-one correspondence" of temperature T and position x, the temperature profile is a continuous and strictly monotonous one (with that a bijective function). This especially applies for maximum η and maximum φ if constant or real, temperature dependent, material properties are considered.[7] Then, there exists an inverse function $x(T)$ corresponding to $T(x)$ and vice versa. If these conditions are fulfilled, Eq. (1.16) can be transformed into

$$\frac{d}{dx}\left(-\kappa(x)\,\frac{dT(x)}{dx}\right) + j\,T(x)\,\frac{d\alpha(x)}{dx} = \frac{j^2}{\sigma(x)} \tag{1.17}$$

---

[7]Within CPM we find for the slope of the temperature profile at the sink side $T'(L) = 0$ for the maximum temperature difference ($\varphi = 0$), and $T'(L) > 0$ for $\varphi > 0$. Note that the CPM is a suitable reference for moderately temperature dependent material properties.

with $\sigma(x) = 1/\rho(x)$. Identical temperature profiles $T(x)$ are calculated from Eqs. (1.16) and (1.17) if spatial material profiles over the length of the TE element are given by $\alpha(x) = \alpha[T(x)]$, $\sigma(x) = \sigma[T(x)]$, and $\kappa(x) = \kappa[T(x)]$.

It is common knowledge that the material properties, especially those of semiconductors, highly depend on the carrier concentration which can be influenced by appropriate doping agents or a variation of the chemical composition [38,39,50,58,75,80,81,86,94,95,106,143,144, 167]. Controlling the carrier concentration gives in principle the opportunity to get a spatially dependent material even if the temperature dependence is neglected [182,183]. This approach can be generalized for FGM. All material parameters may then depend not only on the temperature, but also on the local material quality which can be practically the composition of an alloy or the concentration of a dopant. Symbolically, for example representing the concentration of a single doping species or alloying element, the local material quality can be denoted by a concentration variable c. Thus, the gradient of the Seebeck coefficient α is e.g. [70]

$$\nabla\alpha = \nabla\,\alpha\,|_{T=\text{const}} + \frac{\partial\alpha}{\partial T}\,\nabla T$$

leading to

$$\implies \quad \nabla\alpha(T,c) = \left.\frac{\partial\alpha}{\partial c}\right|_{T=\text{const}} \nabla c + \left.\frac{\partial\alpha}{\partial T}\right|_{c=\text{const}} \nabla T\ .$$

For the 1D case, and the x-coordinate used, the gradient of Seebeck can simply be written as $\nabla\alpha = d\alpha/dx\,\mathbf{e}_x$ if the single element profiles $c(x)$ and $T(x)$ are known:

$$\alpha(x) = \alpha\left[c(x),\,T(x)\right]\ .$$

These considerations have been the reason for establishing the spatial coordinate as the independent coordinate for an empirical approach to 1D, steady-state problems with graded materials. Naturally, Eq. (1.17) can also be used as an independent differential equation when the spatial dependence of the material parameters $\alpha(x)$, $\sigma(x)$, $\kappa(x)$ is of prime interest, see e. g. [18, 107, 108, 154, 157].

We want to remark here that the differential equation (1.16) is nonlinear whereas Eq. (1.17) containing spatial material profiles is linear in T which opens broader opportunities for

finding analytical solutions and applying the principle of superposition.

Once having calculated $T(x)$, all performance parameters of interest can be determined as a function of the electrical current density j, e.g.

- TEG: net power output density[8] (electrical power output per cross-sectional area A_c):

$$p_{\text{net}}(j) = -p(j) = -P(j)/A_c = -\int_0^L \left[\rho(x)\,j^2 + j\,\alpha(x)\,T'(x) \right]\,dx \;,$$

  where P is the electrical power output, p is the corresponding density.

- TEC: cooling power density (absorbed heat per time and cross-sectional area):

$$q_a(j) = Q_a(j)/A_c = \left[-\kappa(x)T'(x) + j\alpha(x)T(x) \right]_{x=0} \;,$$

  where Q_a is the cooling power (absorbed heat per time unit).[9]

- TEG: efficiency $\eta(j) = p_{\text{net}}(j)/q_a(j)$

- TEC: coefficient of performance $\varphi(j) = Q_a(j)/P(j) = q_a(j)/p(j)$.

Concerning notation we refer to [157]. For fixed material profiles (given gradients), the optimum current density can be calculated from the maximum of the device performance. For example, for arbitrary continuous monotonic gradient functions of the material profiles $\alpha(x), \sigma(x)$ and $\kappa(x)$, the calculation of the temperature profile has been done numerically up to now either by a 1D finite element method code (1D TE FEM) or the algorithm of multisegmented elements as well as other approaches, see e.g. [10, 11, 18, 19, 72, 74, 82, 123, 127, 156, 160, 161] and section 1.5.1

There is no doubt that global maximization of a performance parameter of the element as an integral device is a suitable guideline for an empirical approach to numerical device optimization, see e.g. [38, 39]. The target of 1D TE FGM research, however, is to find a set of optimal profiles $\alpha(x), \sigma(x), \kappa(x)$ for maximizing the performance of TE devices. Here we make use of the fact that analytical solutions of the generalized heat equation, Eq. (1.17), can be found for spatially linear material profiles (see section 1.5.2). These can actually be used as the starting point for finding more general optimal material profiles (regarding the profile shape).

---

[8]Power output is defined here according to thermodynamic rules: quantities put into the system are positive.
[9]Note that the dot for the time derivative is often omitted $Q_a \equiv \dot{Q}_a$.

Further on we will refer to the efficiency η of a thermogenerator (TEG) and to the coefficient of performance φ of a Peltier cooler (TEC), because maximization of these global device parameters can be deduced to local optimization, see [159] and section 1.6. The power output (TEG) and the pumped heat (TEC) have to be treated separately (see section 1.8).

1.4 The maximum thermoelectric performance

Throughout thermoelectric modeling, TE performance was initially considered assuming temperature independent materials. The Constant Properties Model (CPM) is an adequate as well as historical reference for comparing both thermoelectric materials and devices.

1.4.1 Maximum performance

The efficiency η of a TEG and the coefficient of performance φ of a Peltier cooler can be calculated from the temperature dependent material parameters of n-type and p-type elements, geometry, current, thermal and electrical contact resistances [166] from suitably defined global averages of TE quantities

Here we define the thermoelectric device figure of merit ZT in contrast to the materials figure of merit zT [60] using the well-known formulae for maximum efficiency and coefficient of performance for constant material properties $[30, 50, 54, 60, 71, 75]$

$$\eta_{\mathrm{max}} = \frac{T_{\mathrm{a}} - T_{\mathrm{s}}}{T_{\mathrm{a}}} \frac{\sqrt{1 + ZT} - 1}{\sqrt{1 + ZT} + T_{\mathrm{s}}/T_{\mathrm{a}}} \tag{1.18a}$$

and

$$\frac{1}{\varphi_{\mathrm{max}}} = \frac{T_{\mathrm{s}} - T_{\mathrm{a}}}{T_{\mathrm{a}}} \frac{\sqrt{1 + ZT} + 1}{\sqrt{1 + ZT} - T_{\mathrm{s}}/T_{\mathrm{a}}} \quad , \tag{1.18b}$$

where $T_{\mathrm{a}} = T_{\mathrm{h}}$ and $T_{\mathrm{s}} = T_{\mathrm{c}}$ for TEG and $T_{\mathrm{a}} = T_{\mathrm{c}}$ and $T_{\mathrm{s}} = T_{\mathrm{h}}$ for TEC. Given a maximum performance value one can subsequently solve for the device figure of merit ZT. For a precise definition, the values of T_{s} and T_{a} as well as whether the device is TEC or TEG must be specified - usually the T in ZT is assumed to be $T_{\mathrm{m}} = 1/2(T_{\mathrm{a}} + T_{\mathrm{s}})$. In general this ZT also depends on the exact temperature dependent materials properties, exact geometry, even including non-idealities such as electrical and thermal losses (e.g. contact resistances, parasitic losses) and non-optimized geometric parameters. However since even the ideal CPM

model requires electrical current optimization to achieve the maximum efficiency determined by ZT, the current should be adjusted (experimentally or theoretically) to achieve maximum efficiency when using this definition of ZT. For an ideal single element without parasitic losses the device ZT is equal to the material's zT within the framework of the CPM.[10]

1.4.2 Approximating effective device figure of merit

For an actual thermoelectric module, where the exact properties, dimensions and interfaces of all the materials involved are not known, exact quantitative description as a device is restricted to the measurable parameters related to the TE material properties α, σ and κ: the device effective Seebeck coefficient α_{eff}, electrical resistance R and thermal conductance K. The exact procedures for measuring $\alpha_{\mathrm{eff}}, K, R$ are not universally accepted [20, 21, 24, 46, 47, 65–67, 69, 76, 77, 83, 86–88, 125, 128, 133, 137–139, 151, 170] and therefore do not give exactly the same results. Nevertheless such values can be used to define an effective $Z_{\mathrm{eff}}T$ as

$$ZT = z_{\mathrm{eff}}T = \frac{\alpha_{\mathrm{eff}}^2 T}{R\,K} \tag{1.19}$$

where it is common to use $T = T_{\mathrm{m}}$. A good thermoelectric material is characterized by a large Seebeck coefficient to produce the thermoelectric voltage, a low thermal conductivity for limiting the dissipative Fourier heat flow throughout the device exposed to a temperature gradient and a low electrical resistivity (high electrical conductance) to minimize Joule's heating. Altogether these conditions are combined into the figure of merit [50, 54, 60, 60, 61, 70, 71, 75, 84, 147–149, 180]. By definition, see Eq. (1.18), two devices with the same ZT (operated under the same conditions) have the same performance. Two devices with the same or similar $Z_{\mathrm{eff}}T$ should reach similar performance to each other under similar conditions (as both TEG and TEC) but they need not be exactly equal.

Physically, it may seem most justified to use averaged materials properties to estimate the effective figure of merit and power factor f_{eff} such as

$$\frac{\alpha_{\mathrm{eff}}^2}{R\,K} = \frac{\alpha_{\mathrm{eff}}^2}{[\rho(x)]_{\mathrm{av}}} \left[\frac{1}{\kappa(x)}\right]_{\mathrm{av}} \quad \text{and} \quad f_{\mathrm{eff}} = \frac{\alpha_{\mathrm{eff}}^2}{[\rho(x)]_{\mathrm{av}}} \, , \tag{1.20}$$

---

[10]The formulae (1.18) can be derived straightforwardly by using Eqs. (9)–(12) in [157], as well as within the symmetric CPM model where the n-leg and p-leg have equal properties with opposite Seebeck coefficients. In [157] you may also find the CPM formulae for the appropriate optimal current densities.

with

$$\alpha_{\text{eff}} = \overline{\alpha}, \quad R = \frac{1}{A} \int \rho(x)\,dx = \frac{L}{A}\,[\rho(x)]_{\text{av}}, \quad \text{and}$$

$$\frac{1}{K} = \frac{1}{A} \int \frac{1}{\kappa(x)}\,dx = \frac{L}{A}\left[\frac{1}{\kappa(x)}\right]_{\text{av}}, \tag{1.21}$$

but also other formulations are used. Note that the overbar in Eq. (1.20) corresponds to the average over temperature. For details of the averaging see next subsection.

1.4.3 Averaging the material profiles

At this point, we refer to a great variety of scientific work in experimentally measuring or determining the temperature dependence of the material coefficients, for an overview see [25, 67, 68, 70, 75, 118, 147, 148, 165, 167, 172, 177] and references therein.

The quantities zT and ZT are used here as single quantities in contrast to the traditional use of z or Z with units of K^{-1} (the traditional "figure of merit"). The dimensionless form is more fundamental with zT always being found together in thermodynamic equations. In CPM calculations, which are often applied for approximating the efficiency or coefficient of performance even for spatial or temperature dependent material profiles (see e.g. [183]), T is a reference temperature or an average of T_{a} and T_{s}. There is no doubt that zT is the "true" figure of merit from the thermodynamic point of view.[11]

As early as in 1957 Ioffe considered that there are mainly two possibilities for averaging TE material properties in devices [75]: firstly, the average over space (denoted with the index "av") and secondly, the average over the temperature scale which is denoted here with an overbar. Both can be related to each other if the temperature profile is monotonous, e. g. for Seebeck

$$\overline{\alpha} = \frac{1}{T_{\text{s}} - T_{\text{a}}} \int_{T_{\text{a}}}^{T_{\text{s}}} \alpha(T)\,dT = \frac{1}{L} \int_{0}^{L} \alpha(x)\,\frac{T'(x)}{(T_{\text{s}} - T_{\text{a}})/L}\,dx$$

$$\approx \frac{1}{L} \int_{0}^{L} \alpha(x)\,dx = \alpha_{\text{av}}\,,$$

---

[11]Note that there is no apparent upper limit to zT although maximum zT has been discussed by several authors [51, 59, 103, 104, 141, 178]. Already Harman and Honig derived $zT < 18$ from the viewpoint of elementary transport theory, see [70] on page 304.

if $\alpha(x) = \alpha[T(x)]$, i.e. if there is no explicit spatial dependence.

Note that $\int_0^L T'(x)\,dx = \int_{T_a}^{T_s} dT = T_s - T_a$; therefore the function $L\,T'(x)/(T_s - T_a)$ varies around unity, and both averages are close together for moderate gradients. Further note that both averages coincide in general for a linear temperature profile, but also for the CPM although it is linked to a particular non-linear profile (parabola). For temperature dependent material Ioffe suggested

$$\rho_{av} = \ln\left(\frac{T_a}{T_s}\right) \int_{T_a}^{T_s} \rho(T)\,\frac{1}{T}\,dT \quad .$$

as an averaging formula for the resistivity. He stated there that the majority of the semi-conductors have $\rho\,T^{-n} =$const. as the temperature dependence of the resistivity. For that you get

$$\rho_{av} = \frac{1}{n}\,\ln\left(\frac{T_a}{T_s}\right)\,(\rho_a - \rho_s) \quad ,$$

see page 62 in [75]. The different averaging procedures are further discussed below in the context of the figure of merit.

For non-planar shaped elements, e.g. ring-shaped elements, see [97–99, 102, 111, 113, 140], where the current flows are not one-dimensional, the product of $R\,K$ is independent of the shape. So does the effective figure of merit, see Eq. (1.19). This can be shown, e.g. with the relation

$$R\,K = \kappa\,\rho = \frac{\kappa}{\sigma}$$

for an ideal single and prismatic element, where the global parameters resistance $R = \rho\,L/A_c$ and thermal conductance $K = \kappa\,A_c/L$ are correlated to the local ones (κ, $\rho = \sigma^{-1}$), see e.g. [54] on p. 127.

Doubtless, a method of approximating the device figure of merit $Z\,T$ from the materials data is necessary for temperature dependent or spatially dependent material to estimate the performance as given above, see Eq. (1.18). Typically averaged values are used. In most cases either all material parameters are taken as temperature dependent (spatially dependent) or all are averaged. Averaging over space might seem adequate as the graded element is considered as a serial connection of segments. On the other hand, averaging over

T is very practicable since it does not require knowledge of the temperature profile but can be simply deduced from temperature dependent material properties.

Formally, z_{av} can be calculated by averaging $\alpha^2 \sigma / \kappa$ locally with respect to temperature or space or from individual averages (over temperature resp. over space) of each material profile which would lead to $z_{\mathrm{av}} = \alpha_{\mathrm{av}}^2 \sigma_{\mathrm{av}} / \kappa_{\mathrm{av}}$ for the purpose of easy analytical treatment. The latter has been done for example by Kaliazin and co-workers [82]. Alternatively, Ioffe [75], Moizhes [119], Borrego [22, 23], and Efremov/Pushkars [49] defined

$$z_{\mathrm{eff}} = \frac{(\overline{\alpha})^2}{\overline{(\rho \, \kappa)}} = \frac{\left(\int_{T_{\mathrm{a}}}^{T_{\mathrm{s}}} \alpha(T) \, dT \right)^2}{(T_{\mathrm{s}} - T_{\mathrm{a}}) \int_{T_{\mathrm{a}}}^{T_{\mathrm{s}}} \rho(T) \, \kappa(T) \, dT} \; , \tag{1.22}$$

an averaging which we also recommend for purely temperature dependent material properties. The formula is obtained starting with the calculation of the temperature distribution for the idle case ($j = 0$), where you find from the thermal energy balance (1.16) that the heat flux is a constant and it follows that

$$q \, L = \int_0^L \kappa \frac{dT}{dx} \, dx = \int_{T_{\mathrm{a}}}^{T_{\mathrm{s}}} \kappa(T) \, dT = \overline{\kappa} \, \Delta T,$$

where $\Delta T = T_{\mathrm{s}} - T_{\mathrm{a}}$.[12] So you find in the absence of a current that the heat flux becomes

$$Q = \overline{\kappa} \, A_{\mathrm{c}} \frac{\Delta T}{L} = K \, \Delta T \Rightarrow K = \overline{\kappa} \frac{A_{\mathrm{c}}}{L} \; .$$

The overall resistance of the TE element can be easily obtained

$$R = \frac{L}{A_{\mathrm{c}}} \rho_{\mathrm{av}} = \frac{1}{A_{\mathrm{c}}} \int_0^L \rho(x) \, dx = \frac{1}{A_{\mathrm{c}}} \int_{T_{\mathrm{a}}}^{T_{\mathrm{s}}} \rho(T) \frac{dx}{dT} \, dT$$

$$= \frac{L}{\overline{\kappa} \, A_{\mathrm{c}}} \frac{1}{\Delta T} \int_{T_{\mathrm{a}}}^{T_{\mathrm{s}}} \rho(T) \, \kappa(T) \, dT$$

$$\Rightarrow R = \frac{\overline{\rho \, \kappa}}{\overline{\kappa}} \frac{L}{A_{\mathrm{c}}}.$$

Thus we find for the locally averaged resistivity $\rho_{\mathrm{av}} = \overline{\rho \kappa} / \overline{\kappa}$ which is nothing else than a weighted average of the (temperature dependent) resistivity by the (temperature depen-

---

[12]Note that the sign of ΔT can be both positive or negative depending on how the TE element operates (TEG/TEC).

dent) thermal conductivity. The product RK is then the temperature average over the product of (temperature dependent) resistivity and thermal conductivity $\overline{\rho\kappa}$. It is stated by the authors [23, 49, 75, 119, 184] that Eq. (1.22) is valid only for the zero current limit but the use of these averaged properties still results in meaningful estimates of the device performance. Of course the exact method is to calculate the performance as described in section 1.4.1

Min and co-workers also highlighted a method to calculate an effective $Z_{\text{eff}} T$, especially if large temperature differences are present [116].

The concept of effective figure of merit and power factor had been discussed in the framework of composite materials as the so called *effective medium theory* [15–17,73,85,96,164,171,181]. In all of these cases a random distribution of different materials is supposed. It was found that this can enhance the power factor but not the efficiency of the TE material. This is clearly different from the situation as discussed here where we haven't got a random inhomogeneity but a directed grading or segmentation.

1.5 Model-free setup based on spatial material profiles

In this section, a setup is used where an independent and free variability of the spatial material profiles $\alpha(x)$, $\sigma(x)$ and $\kappa(x)$ is assumed primarily, and where the temperature profile $T(x)$ can be calculated directly from Domenicali's thermal energy balance [45]. Formula (1.17) is rewritten here as

$$\kappa(x)\,T''(x) + \kappa'(x)\,T'(x) - j\,\alpha'(x)\,T(x) = -\rho(x)\,j^2 \ . \tag{1.23}$$

Once knowing $T(x)$, all application-relevant device properties and performance parameters can be derived. Executing the calculation in a loop while varying the current allows to select optimum operation parameters (optimum load resistance and current, resp.) and deduce maximum performance values.

The aim of such investigations is to identify optimum combinations of material gradients along a graded generator or cooler element. However, the practical accessibility of optimum gradient schemes is limited by the constraint of maximum zT of available materials, by the

magnitude of the compositional gradient (extremely steep profiles are difficult to prepare in a controlled manner), and by interrelations between the thermoelectric properties due to the solid state nature of the TE materials, for example, the Wiedemann-Franz law connecting electronic part of thermal conductivity and electrical conductivity.

1.5.1 Parameter studies via numerical calculations

Fundamental parameter studies [123, 126] have demonstrated quantitative improvement of performance achievable by material grading. Numerical calculations were based on the afore-mentioned model-free setup applying arbitrarily but suitably chosen continuous monotonic gradient functions for all material profiles (see e.g. [124])

$$y(x) = y_\mathrm{a} + \frac{1 - \exp(k_y\, x/L)}{1 - \exp(k_y)}(y_\mathrm{s} - y_\mathrm{a})\,, \quad y = \alpha,\, \sigma,\, \kappa \tag{1.24}$$

which fix the values y_a and y_s at the absorbing and sink side, resp., but allow to vary the curvature by the numerical parameter k_y. It was found that best performance is achieved close to linear profiles in certain cases (see Fig. 1.3), whereas an unfavorable combination of slopes such as strong gradients of α and σ oriented in parallel lead to a significant drop of the performance. Further it is worth mentioning that, related to the higher optimum
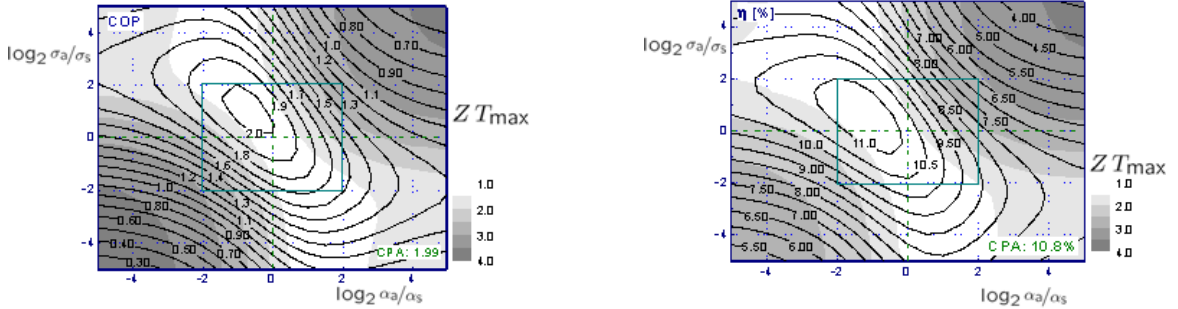

Figure 1.3: Variation of the maximum φ of a TEC for $T_\mathrm{a} = 280$ K, $T_\mathrm{s} = 300$ K (left) and maximum efficiency of a TEG for $T_\mathrm{a} = 600$ K, $T_\mathrm{s} = 300$ K (right) plotted versus the chosen constant gradients of the Seebeck coefficient and electrical conductivity (see also [123]); under the constraint of $(z\,T)_\mathrm{av} = \mathrm{const.}$; double-logarithmic plot: $\log_2(\alpha_\mathrm{a}/\alpha_\mathrm{s})$ (abscissa), $\log_2(\sigma_\mathrm{a}/\sigma_\mathrm{s})$ (ordinate) in both figures; The inner frame marks the region of small to moderate gradients. The gray-tone background indicates the maximum $z\,T$ which is found locally within the respective gradient configuration. For the calculation we chose $\alpha_\mathrm{av} = 180$ µV/K, $\sigma_\mathrm{av} = 140000$ S/m and κ_av such that the spatial average of the figure of merit is unity, i.e. $(z\,T)_\mathrm{av} = 1$.

current density, achievable effects are larger for Peltier coolers than for a TEG although the

operating temperature difference was assumed much larger for generators. The strongest improvement for Peltier elements can be achieved at the maximum temperature difference if steep material gradients are selected. Concerning a detailed discussion we refer to [123,126].

1.5.2 Analytical solution based on linear material profiles

Variation restricted to linear spatial material profiles provide hints to favorable configurations of material profiles that deliver optimum performance. The linear properties model (LPM) is – as well as the constant properties model (CPM) – of course limited in comparison with real temperature dependent materials, but it can give hints, e. g. for optimized stacking schemes.

Investigations based on linear spatial profiles have already been done in the mid-1960's by Ybarrondo et al. [182,183]. Although they could give an analytical solution for the temperature profile (for a TE cooler with mixed boundary conditions), the performance couldn't be determined quantitatively by them due to the lack of suitable computation tools. Therefore we revisit the corresponding solutions in particular to gain information about the influence of the slope of the material parameters on the performance, and we calculate the corresponding optimal values in our particular case of linear spatial profiles as an interesting example of FGM.

Assuming linear profiles, the thermal energy balance (1.23) can be written in the notation

$$[a(\kappa)\ \xi_\kappa + b(\kappa)\,x]\ T''(x) + b(\kappa)\,T'(x) - j\,b(\alpha)\,T(x)$$
$$= -j^2\,[a(\sigma)\,\xi_\sigma + b(\sigma)\,x]^{-1} \tag{1.25}$$

using the abbreviations

$$\xi_y = \frac{y_a}{y_s},\ a(y) = \frac{2\,y_{\mathrm{av}}}{1 + \xi_y}, \quad \text{and} \quad b(y) = \frac{2\,y_{\mathrm{av}}}{L}\,\frac{(1 - \xi_y)}{(1 + \xi_y)} = \frac{\Delta y}{L}$$

with $y = \kappa, \sigma, \alpha$. It is obvious that b gives the appropriate slope of the material profile, e. g. $\kappa'(x) = b(\kappa)$. As free parameters for the linear profiles of the material we chose the fixed spatial average y_{av} to compare with CPM and the grading parameters ξ_y. Note that there is another form of writing the material profiles with the chosen abbreviations, e. g. $\kappa = a(\kappa)\,\xi_\kappa + b(\kappa)\,x$, with $\xi_\kappa = \frac{\kappa_{\mathrm{a}}}{\kappa_{\mathrm{s}}}$ being a primary characteristics of the linear profile. To

get the Bessel equation from the homogeneous part of the thermal energy balance we further use the substitution

$$w(x) = -2\sqrt{\frac{-j\,b(\alpha)}{b^2(\kappa)}}\,\sqrt{\kappa(x)}$$

$$= -2L\sqrt{\frac{j(\alpha_a - \alpha_s)}{L(\kappa_s - \kappa_a)^2}}\,\sqrt{\kappa(x)} \equiv A\,\sqrt{\kappa(x)} \tag{1.26}$$

leading to $T''(w) + w^{-1}\,T'(w) + T(w) = 0$ for the homogeneous part of Eq. (1.25) which is equivalent to a Bessel differential equation of order 0 (after multiplying with w^2). The completely transformed inhomogeneous differential equation is finally [186]

$$T''[w(x)] + w^{-1}(x)\,T'[w(x)] + T[w(x)] = \frac{j}{b(\alpha)\,\sigma_{\mathrm{av}}}\ . \tag{1.27}$$

The temperature profile is found in terms of Bessel functions $Y_0(w)$, $J_0(w)$ with w given by Eq. (1.26) for the general case $\xi_\alpha \neq 1$, $\xi_\sigma \neq 1$, $\xi_\kappa \neq 1$

$$T(x) = C_1\,Y_0[w(x)] + C_2\,J_0[w(x)] +$$

$$\frac{\pi j^2 L}{\Delta\kappa}\left[J_0[w(x)]\int_0^L \frac{Y_0[w(x)]}{\sigma(x)}\,dx - Y_0[w(x)]\int_0^L \frac{J_0[w(x)]}{\sigma(x)}\,dx\right]\ . \tag{1.28}$$

The free constants C_1 and C_2 can be fixed according to the given boundary conditions. For an overview on Bessel functions we refer to standard textbooks [1, 109]. The tables of all particular solutions of Eq. (1.27) are given in the appendix of [186].

Although the CPM as well as the LPM cases appear physically simple, these are not at all simple from the point of view of materials' fabrication [38, 39, 94, 95]; the question how to obtain TE materials with linear material profiles is still an open issue.

1.5.3 TEG performance optimization via linear grading

Once the temperature profile $T(x)$ throughout an element has been calculated, the performance parameter, e.g. power output density p and efficiency η of a thermogenerator depending on the electrical current density j and the grading parameters ξ_α, ξ_σ and ξ_κ can be determined and can consequently be optimized according to the variation of these. Considering power output here, we find Eq. (1.29) for a constant electrical conductivity ($\xi_\sigma = 1$), which is supposed to be in the vicinity of the maximal performance, after integration by

parts [185]

$$p \equiv p(j, \xi_\alpha, \xi_\kappa) = -\frac{j^2\, L}{\sigma_{\mathrm{av}}} - j\,\frac{2\,\alpha_{\mathrm{av}}}{1 + \xi_\alpha}\,[T_{\mathrm{s}} - T_{\mathrm{a}}\,\xi_\alpha - (1 - \xi_\alpha)\,T_{\mathrm{av}}] \tag{1.29}$$

with $T_{\mathrm{av}} = L^{-1} \int_0^L T(x)\,dx$. In Eq. (1.29) the grading of κ enters through that spatial average of the temperature T_{av}. Here, the particular case of having only one linear profile for the Seebeck coefficient ($\xi_\alpha \neq 1$) shall be shortly discussed. For that the material parameters are chosen as $\alpha_{\mathrm{av}} = 180\ \mu\mathrm{V/K}$, $\kappa_{\mathrm{av}} = 1.35\ \mathrm{W/m\,K}$ and $\sigma_{\mathrm{av}} = 140000\ \mathrm{S/m}$, exemplarily. Thus $z\,T$ at $T = 300$ K equals approximately 1. In the CPM case, a simple extremal problem to get optimum current densities j_{opt} leading to the optimal value of the performance parameter p_{max} and η_{max} has to be solved, whereas for LPM one ends up with a multidimensional extremal problem with a system of equations leading to the optimum current densities j_{opt} and grading parameters ξ_{opt}. Both TEG performance parameters are displayed in the
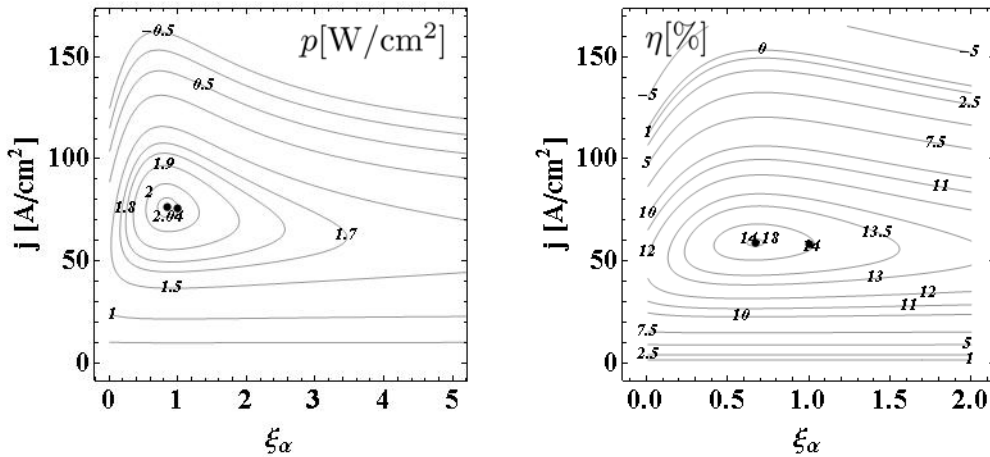
Figure 1.4: Performance parameter in dependence of j and ξ_α for $T_{\mathrm{a}} = 600$ K and $T_{\mathrm{s}} = 300$ K, $L = 5$ mm. The other two grading parameters ξ_κ and ξ_σ are set to unity, i.e. σ and κ are constant; left: electrical power output density p in $\mathrm{W/cm}^2$, right: efficiency η in %. In comparison to Fig. 1.3 there is no constraint for $z\,T$ in this calculation. We fixed the material parameters to $\alpha_{\mathrm{av}} = 180\ \mu\mathrm{V/K}, \sigma_{\mathrm{av}} = 140000\ \mathrm{S/m}$ and $\kappa_{\mathrm{av}} = 1.35\ \mathrm{W/m\,K}$.

Fig. 1.4 for a TE element of length $L = 5$ mm and a temperature difference of $\Delta T = 300$ K. The results for CPM and LPM are compared in table 1.1.

By linear grading of α both the power output and the efficiency can be slightly increased. As for CPM the optimal parameters are different, depending on what has to be optimized, p or η, but we find the same tendency in the optimization strategy. Obviously, there is only a slight increase when assuming $\kappa =$ const.; with linear profiles $\alpha(x)$ and $\kappa(x)$ the increase of power output and efficiency in the TEG case is more pronounced, see [185–187].

The same effect is expected for the TEC case with linear profiles $\alpha(x)$ and $\sigma(x)$. Note that

Table 1.1: Values of the optimum performance parameters for the given material

	Maximum output power output density			Maximum efficiency		
	$j_{\mathrm{p,opt}}[\mathrm{A/cm^2}]$	$\xi_{\alpha,\mathrm{opt}}$	$p^{\max}[\mathrm{W/cm^2}]$	$j_{\eta,\mathrm{opt}}[\mathrm{A/cm^2}]$	$\xi_{\alpha,\mathrm{opt}}$	$\eta^{\max}[\%]$
CPM	75.6	1	2.041	58.5	1	14.03
LPM	76.1	0.85	2.048	59.0	0.67	14.19

all of these conclusions are found supposing fixed spatial averages of α, σ and κ as a limit to the material performance. Hence, in the light of the following has to be mentioned that the optimum configurations which exceed the CPM in performance are bound to a slightly higher z_{eff}, see Eq. (1.20), than in the CPM case. This applies both to the results given in Figs. 1.3 and 1.4. The observed non-symmetry is mainly founded in the non-symmetric contribution of α (squared) and σ (linear) to the figure of merit. This is another, numerical evidence on the conclusion of section 1.4.2 and 1.4.3 that fixing the spatial averages of α, σ and κ is not a physically justified reference of "equally good" material, neither is the fixing of the spatial average of $z\,T$ as was applied in the calculations for Fig. 1.3.

1.6 Compatibility approach and optimum material grading

In 2002/2003 Snyder and Ursell [168,169,176] introduced the *compatibility factor* as a second characteristic besides the $z\,T$ for optimizing the performance of TE devices. By introducing the relative current density u and the reduced efficiency η_{r} (see Section 1.2), the thermoelectric power generation could be formulated at first at the level of intensive state variables. Building on earlier investigations dating from the 1960's [35, 50, 70, 120, 135, 160, 174, 183], this concept has been further developed in successive works [53, 100, 101, 155–157] on the basis of a one-dimensional, stationary and unifying model with material grading for the thermogenerator and the Peltier cooler.

The compatibility approach is an alternative to Ioffe's description using global power terms which is very often used for technological applications, but is certainly not suitable for locally characterizing TE processes or even for local optimization purposes.

The advantage of using the relative current density is that the multidimensional TE problem can be reduced to a one-dimensional heat flow problem[13] formulated in $u(T)$ where the

---

[13] For the history of local definition of efficiency see also [120]; in [64] the three-dimensional vector version is presented. A more general definition of u seems possible when writing the relative current density in terms of fluctuating currents which are indeed 3D.

governing equation can be evaluated from the thermal energy balance [168]

$$\frac{d}{dT}\left(\frac{1}{u}\right) = -T\frac{d\alpha}{dT} - u\rho\kappa \quad \text{or} \quad u'(T) = \tau\,u^2 + \rho\kappa\,u^3 \,, \tag{1.30}$$

alternatively, with the Thomson coefficient $\tau(T) = T\,d\alpha/dT$. Basically, Eq. (1.30) describes a homogeneous TE element with temperature dependent material properties, whereby (1.30) holds for both the "pump up" ($T'(x) > 0$) and "pump down" ($T'(x) < 0$) cases.[14] Further note that TEG and TEC cases are only distinguished by the sign of $u(T)$ if the same (temperature dependent) material properties, the same current density, but reversed boundary temperatures T_a and T_s are applied ($T_\mathrm{a} > T_\mathrm{s}$ for TEG, but $T_\mathrm{a} < T_\mathrm{s}$ as usual for TEC). Meanwhile it has been shown that sufficient compatibility is – besides a high figure of merit z_eff – essential for efficient operation of a TE device, and that compatibility will facilitate rational materials selection, device design and FGM engineering, see e.g. [53, 100, 101, 127, 165, 166, 176]. Currently, compatibility factors $s = u_\mathrm{opt}$ are available for performance parameters arising from the local contribution to the TE material; these are:

- TEG: compatibility factor for maximal electric power ($s^{(\mathrm{g,P})}$ or $s^{(\mathrm{P})}$) [155]: $s^{(\mathrm{P})} = \frac{z}{2\alpha}$

- TEG: compatibility factor for maximal η ($s^{(\mathrm{g})}$) [168]:
  $s^{(\mathrm{g})} = \frac{\sqrt{1+zT}-1}{\alpha T}$

- TEC: compatibility factor for maximal φ ($s^{(\mathrm{c})}$) [156]:
  $s^{(\mathrm{c})} = \frac{-\sqrt{1+zT}-1}{\alpha T}$

The importance of the compatibility approach has been demonstrated first for a segmented thermoelectric generator [166, 168, 176]. Snyder pointed out that, if the compatibility factors in segmented devices with given material differ by a factor of 2 or more, the maximum efficiency of a TEG can in fact decrease by segmentation. Compatibility is therefore of essential importance for a rational material selection in segmented devices.

Alternatively, compatibility can be considered in the same material [168, 169, 176]. One of the major objectives in FGM research is to find optimal graded TE elements [so called self-compatible elements, where $u(x) \approx s(x)$] to achieve maximum performance. Sherman and co-workers [160] referred to perfectly infinitely staged material which gives the maximum efficiency or coefficient of performance. Within the new concept of self-compatibility the

---

[14]Erratum: [156] Eq. (9), right hand side, the $\pm$ sign has to be replaced by a minus sign valid for both the pump up and the pump down situation.

guidelines toward a perfectly infinitely staged, i.e. ideally self-compatible material are now well defined. However because both zT and s depend on the same materials parameters, a compromise between high zT and self-compatibility will need to be reached for true optimization. Example calculations of self-compatible elements for maximum η (TEG) and maximum φ (TEC) are presented in Section 1.6.2, concerning power-related compatibility see section 1.8.

1.6.1 FGM and self-compatibility

The exact solution for η and φ with respect to temperature, i.e. for temperature dependent material parameters are the following integrals taken from [159] for TEG:

$$\ln(1 - \eta) = \int_{T_{\mathrm{a}}}^{T_{\mathrm{s}}} K(u(T), T)\, dT \quad \text{with} \quad T_{\mathrm{s}} \leq T \leq T_{\mathrm{a}}\ , \tag{1.31a}$$

and for TEC

$$\ln\left(1 + \frac{1}{\varphi}\right) = \int_{T_{\mathrm{a}}}^{T_{\mathrm{s}}} K(u(T), T)\, dT \quad \text{with} \quad T_{\mathrm{a}} \leq T \leq T_{\mathrm{s}}\ , \tag{1.31b}$$

where we have one kernel $K(u(T), T)$ for integrals of both generator and cooler

$$\begin{aligned} K(u, T) &= \frac{1}{T}\, \eta_{\mathrm{r}}(u, T) = \frac{1}{T}\frac{1}{\varphi_{\mathrm{r}}(u, T)} = \frac{1}{T}\frac{u\frac{\alpha}{z}\left(1 - u\frac{\alpha}{z}\right)}{u\frac{\alpha}{z} + \frac{1}{zT}} \\ &= \frac{\alpha}{z}\frac{(z - u\alpha)}{(u^{-1} + \alpha T)}\ . \end{aligned} \tag{1.32}$$

Note that K contains the reduced efficiencies η_{r} for TEG resp. φ_{r} for TEC. Alternatively, the integral kernel K can be formulated with the TE potential Φ, see Eq. (1.12). For this case, Snyder [166,168] has shown that η is simply given by the relative change of the thermoelectric potential with temperature variation; an analogous relation can be found for the coefficient of performance (see [156])

$$\eta = 1 - \frac{\Phi(T_{\mathrm{s}})}{\Phi(T_{\mathrm{a}})} \quad \text{and} \quad \varphi = \left(\frac{\Phi(T_{\mathrm{s}})}{\Phi(T_{\mathrm{a}})} - 1\right)^{-1}\ . \tag{1.33}$$

This result points to the importance of the TE potential as a function of state, for details see also [63].

If we assume the feasibility to achieve complete self-compatibility (infinite staging) we can

apply $u = s^{(\mathrm{g})}$ and $u = s^{(\mathrm{c})}$ to the integrals (1.31a) and (1.31b), respectively, so that they take their maximal values with the optimal reduced efficiency $\eta_{\mathrm{r,opt}} = \varphi_{\mathrm{r,opt}} = \frac{\sqrt{1+z\,T}-1}{\sqrt{1+z\,T}+1}$ for both TEG and TEC [75, 160]. Then fully self-compatible performance parameters η_{sc} and φ_{sc} are given by

$$\ln(1 - \eta_{\mathrm{sc}}) = \int_{T_{\mathrm{a}}}^{T_{\mathrm{s}}} \frac{\eta_{r,\mathrm{opt}}}{T}\, dT = \int_{T_{\mathrm{a}}}^{T_{\mathrm{s}}} \frac{1}{T} \frac{\sqrt{1+zT}-1}{\sqrt{1+zT}+1}\, dT \tag{1.34a}$$

and

$$\ln\left(1 + \frac{1}{\varphi_{\mathrm{sc}}}\right) = \int_{T_{\mathrm{a}}}^{T_{\mathrm{s}}} \frac{1}{T\varphi_{\mathrm{r,opt}}}\, dT = \int_{T_{\mathrm{a}}}^{T_{\mathrm{s}}} \frac{1}{T} \frac{\sqrt{1+zT}+1}{\sqrt{1+zT}-1}\, dT \tag{1.34b}$$

or, using Sherman's notation[15] [160]

$$\eta_{\mathrm{sc}} = 1 - \exp\left(-\int_{T_{\mathrm{s}}}^{T_{\mathrm{a}}} \frac{1}{T} \frac{\sqrt{1+z\,T}-1}{\sqrt{1+z\,T}+1}\, dT\right) \tag{1.35a}$$

and

$$\varphi_{\mathrm{sc}} = \left[\exp\left(\int_{T_{\mathrm{a}}}^{T_{\mathrm{s}}} \frac{1}{T} \frac{\sqrt{1+z\,T}+1}{\sqrt{1+z\,T}-1}\, dT\right) - 1\right]^{-1} . \tag{1.35b}$$

We expressly emphasize, however, that the integrals (1.34) and (1.35) do not have extremal properties concerning the $z\,T$ value. Analytical expressions of these integrals can be found for $z = \mathrm{const.}$ as well as for $z\,T = \mathrm{const.}$; a summary of all integral approximations is presented in the appendix of [159]. The constraint $z\,T = \mathrm{const.}$ has proven to be advantageous for the construction of self-compatible elements, see next section.

By using the transformation $\int_{T_{\mathrm{a}}}^{T_{\mathrm{s}}} dT = \int_0^L T'(x)\, dx$ with a monotonous $T(x)$, we find equivalent integrals with the kernel related to the spatial coordinate

$$K^{\star}(u(x), x) = K\left[u(T(x)), T(x)\right] T'(x) . \tag{1.36}$$

Analogous results are obtained from both formulations if $\alpha(x) = \alpha[T(x)]$, $\sigma(x) = \sigma[T(x)]$ and $\kappa(x) = \kappa[T(x)]$.

The integral representations for η and φ have been discussed in [159] within the framework of variational calculus. It was found that the optimal u can only be transferred from T to

---

[15]Note that Sherman et al. used the function $\epsilon(T)$ to denote the optimal reduced efficiency.

x and vice versa if the optimal (and monotonous) temperature profile is known; the latter must be consistent if $u(x) = s(x)$ has to be fulfilled locally. Then, fully self-compatible performance parameters η_{sc} and φ_{sc} are given with the integral kernel $K^{\star}$ (see Eq. (1.36)) by the integrals

$$\ln(1 - \eta_{\text{sc}}) = \int_{0}^{L} K^{\star}(s^{(\text{g})}(x), x) \, dx \tag{1.37a}$$

and

$$\ln\left(1 + \frac{1}{\varphi_{\text{sc}}}\right) = \int_{0}^{L} K^{\star}(s^{(\text{c})}(x), x) \, dx \ . \tag{1.37b}$$

These considerations implicate that two strategies can be established to achieve Snyder's criterion $u = s$ in a local sense, as the condition of self-compatibility, for all infinitesimal segments of a TE element (within the interval $0 \leq x \leq L$ or $T_{\text{a}} \leq T \leq T_{\text{s}}$):

A) optimization based on Eq. (1.30) and the criterion $u(T) = s(T)$, mainly used for temperature dependent materials,

B) optimization based on Eq. (1.23) and the criterion $u(x) = s(x)$ for FGM containing an explicit dependence of the properties on x.

Consistent optimization results are obtained if equivalent material profiles are used. However, it is important to note that constraints or a performance limit must be regarded as well, see Section 1.6.2 for an example.

A central problem is that only two governing equations are available for both optimization strategies when referring to thermoelectricity from a phenomenological point of view. They are, in general, not sufficient for calculating all three optimal material profiles. In addition, the temperature profile $T(x)$ has to be calculated in a consistent manner when $u(x) = s(x)$ is used as (thermodynamic) optimization criterion; it can be rewritten as a first order differential equation for the optimum temperature profile based on the "coordinate" $z \, T$ [157]

$$\frac{dT}{dx} = \frac{j_o}{\sigma \alpha} \, f(z \, T) \quad \text{with} \quad f(z \, T) = \frac{z \, T}{1 \pm \sqrt{1 + z T}} \ . \tag{1.38}$$

The positive sign applies to the TEC ($f = f^{(c)}$), but the negative one to the TEG ($f = f^{(g)}$). An optimization strategy referring to item B) has been proposed in [157]. It has become apparent that self-compatible elements can only be constructed based on an optimum combination of material profiles whereas there is not only a single, uniquely defined set of $\alpha(x), \sigma(x)$, and $\kappa(x)$ but a manifold with two degrees of freedom. Only one profile out of the three properties can be calculated based on the optimization criterion found while two material profiles can be specified arbitrarily to fix an optimum set. The remaining degrees of freedom can be used, e. g., to involve interrelations between the thermoelectric properties due to solid state nature of the TE materials. This strategy has been tested in [157] with presumed constant gradients of α and σ having opposite directions, and the thermal conductivity κ has been optimized.

From first results published in [157] it can be concluded that there is only a little reserve for TEG performance improvement when using optimized material gradients, but much more potential for the performance improvement of a TEC. However, we should emphasize here that the choice of the given profiles determines greatly the increase in performance from the effect of the self-compatibility: Optimization should be based on preset profiles $\alpha(x)$ and $\kappa(x)$ for TEG, but on profiles $\alpha(x)$ and $\sigma(x)$ for TEC. In any case, an ultimate performance limit has to be set, for example by a $z_{\max}(T)$ curve or by a constraint $z = $ const. or $z\,T = $ const., resp., whereby the constant should be related to an average of the figure of merit z or $z\,T$, if direct comparison to a real material shall be made.

The number of predefined profiles can be reduced to only one, when the $z\,T$ constraint is applied, while an important fact is that this constraint may not be realistic from the point of view of materials' actual availability or preparation.

1.6.2 Self-compatible elements for maximum η and maximum φ

Throughout this section, a constant dimensionless figure of merit $z\,T = k_0 = $ const. is assumed. Then, the optimal reduced efficiency is also a constant[16]

$$\eta_{\mathrm{r,opt}} = \varphi_{\mathrm{r,opt}} = \frac{\sqrt{1 + z\,T} - 1}{\sqrt{1 + z\,T} + 1} \quad \Longrightarrow \quad \eta_{\mathrm{r0}} = \frac{\sqrt{1 + k_0} - 1}{\sqrt{1 + k_0} + 1} \ ,$$

---

[16]Note that we use only one constant η_{r0} for both TEG and TEC without distinction, because they are identical $\eta_{\mathrm{r0}} = \varphi_{\mathrm{r0}}$.

and the ideally self-compatible performance parameters η_{sc} for TEG and φ_{sc} for TEC are given by [159]

$$1 - \eta_{sc} = \left(\frac{T_s}{T_a}\right)^{\eta_{r0}} \quad \text{for TEG, and} \quad 1 + \frac{1}{\varphi_{sc}} = \left(\frac{T_s}{T_a}\right)^{1/\eta_{r0}} \quad \text{for TEC.} \tag{1.39}$$

Further, we define here $\eta_{r0} = -\omega_{0,g}/\omega_{0,c}$ with $\omega_{0,g} = \sqrt{1 + k_0} - 1$ for TEG and $\omega_{0,c} = -(\sqrt{1 + k_0} + 1)$ for TEC. Eq. (1.30) shall be evaluated now for the optimal $u_{opt} = s$. Note that the material is represented in Eq. (1.30) by $\alpha(T)$ and the product $\rho(T)\kappa(T)$; both can be optimized based on the constraint $z\,T = k_0$. Applying the compatibility factor $s^{(g)}$ resp. $s^{(c)}$, we find

$$\frac{1}{u} \equiv \frac{1}{s^{(g)}} = \frac{\alpha\,T}{\omega_{0,g}} \quad \text{for TEG} \quad \text{and} \quad \frac{1}{u} \equiv \frac{1}{s^{(c)}} = \frac{\alpha\,T}{\omega_{0,c}} \quad \text{for TEC.} \tag{1.40}$$

The left-hand side of Eq. (1.30) is then for TEG

$$\begin{aligned}
\frac{d}{dT}\left(\frac{1}{u}\right) &\equiv \frac{d}{dT}\left(\frac{1}{s^{(g)}}\right) = \frac{d}{dT}\left(\frac{\alpha\,T}{\omega_{0,g}}\right) \\
&= \frac{1}{\omega_{0,g}}\frac{d}{dT}(\alpha\,T) = \frac{1}{\omega_{0,g}}\left[\alpha + T\frac{d\alpha}{dT}\right]
\end{aligned} \tag{1.41}$$

and for TEC

$$\begin{aligned}
\frac{d}{dT}\left(\frac{1}{u}\right) &\equiv \frac{d}{dT}\left(\frac{1}{s^{(c)}}\right) = \frac{d}{dT}\left(\frac{\alpha\,T}{\omega_{0,c}}\right) \\
&= \frac{1}{\omega_{0,c}}\frac{d}{dT}(\alpha\,T) = \frac{1}{\omega_{0,c}}\left[\alpha + T\frac{d\alpha}{dT}\right] \quad .
\end{aligned} \tag{1.42}$$

For the right-hand side, the definition of the figure of merit gives together with the constraint

$$z = \frac{\alpha^2\,\sigma}{\kappa} = \frac{\alpha^2}{\rho\,\kappa} \quad \implies \quad \rho\,\kappa = \frac{\alpha^2}{z} = \frac{\alpha^2\,T}{k_0} \quad , \tag{1.43}$$

so that we have $s_g\,\rho\,\kappa = \omega_{0,g}\,\alpha/k_0$ for TEG, and $s_c\,\rho\,\kappa = \omega_{0,c}\,\alpha/k_0$ for TEC.

Thus, for both cases, the differential equation for the optimum Seebeck profile $\alpha(T)$ is given by

$$\frac{1}{\omega_0}\left[\alpha + T\frac{d\alpha}{dT}\right] = -T\frac{d\alpha}{dT} - \frac{\omega_0\,\alpha}{k_0} \quad , \tag{1.44}$$

where $\omega_0 \equiv \omega_{0,\mathrm{g}}$ for TEG and $\omega_0 \equiv \omega_{0,\mathrm{c}}$ for TEC, respectively.

Eq. (1.44) can be solved by separation of variables to get a power-law behavior for the optimal Seebeck coefficient where $\alpha_{\mathrm{ref}} = \alpha(T_{\mathrm{ref}})$:

$$\text{TEG:} \quad \alpha(T) = \alpha_{\mathrm{ref}} \left[\frac{T}{T_{\mathrm{ref}}} \right]^{k_{\mathrm{g}}}$$

with

$$k_{\mathrm{g}} = -2\,\frac{\omega_{0,\mathrm{g}}}{k_0} = \frac{2\left(1 - \sqrt{1 + k_0}\right)}{k_0} = \eta_{\mathrm{r}0} - 1 \tag{1.45a}$$

$$\text{TEC:} \quad \alpha(T) = \alpha_{\mathrm{ref}} \left[\frac{T}{T_{\mathrm{ref}}} \right]^{k_{\mathrm{c}}}$$

with

$$k_{\mathrm{c}} = -2\,\frac{\omega_{0,\mathrm{c}}}{k_0} = \frac{2\left(1 + \sqrt{1 + k_0}\right)}{k_0} = \frac{1}{\eta_{\mathrm{r}0}} - 1 \tag{1.45b}$$

As a result, this optimization strategy provides an analytical expression for the optimum Seebeck profile $\alpha(T)$ for both TEG and TEC. Note that the differences in the optimum Seebeck profiles for TEG are marginal for different values k_0 (see Fig. 1.5, left side), and that $\alpha(T)$ is only slightly curved especially for the small temperature interval ($\triangle T = 20$ K) shown for TEC in Fig. 1.5, right side. With given Seebeck coefficient, a second expression is found for the product $\rho(T)\,\kappa(T) = T\alpha^2(T)/k_0$ (see Fig. 1.6), whereas an infinite number of profiles $\kappa(T)$ and $\rho(T) = 1/\sigma(T)$ can be found which fulfill the optimal $\rho(T)\kappa(T)$ product. Notice that these optimization results are valid for a homogeneous element which is described by Eq. (1.30) based on temperature dependent material parameters. For that reason, the results presented here are only suitable for FGM in limited circumstances when further local contributions to the material properties are marginal. In this case, the optimal spatial Seebeck profile $\alpha(x) = \alpha(T(x))$ is increasing with increasing coordinate x for both TEC and TEG as the temperature profile $T(x)$ calculated from Eq. (1.16) is increasing in the TEC but decreasing in the TEG.

Within optimization strategy B, an optimal $T(x)$ can be found from Eq. (1.38) together with one optimal set of spatial profiles. Specifics are discussed here using the constraint $z(x)\,T(x) = k_0 = $ const. whereby fully self-compatible performance values are given again
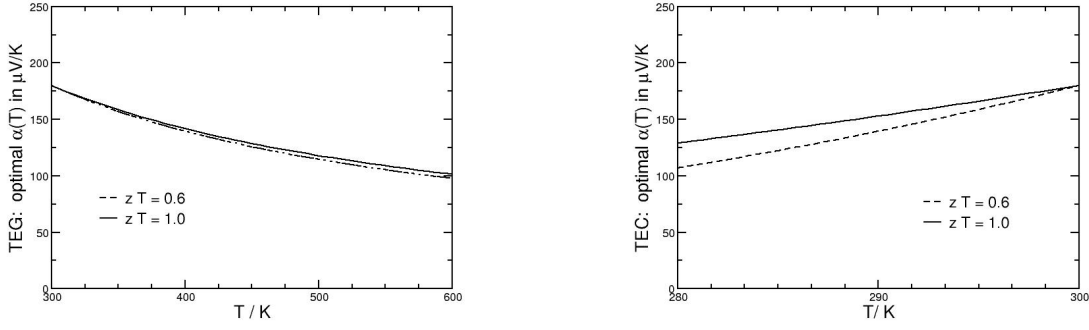
Figure 1.5: Optimal profile of the Seebeck coefficient for TEG (left side, $T_a = 600$ K, $T_s = 300$ K) and TEC (right side, $T_a = 280$ K, $T_s = 300$ K) plotted over temperature for the constraints $zT = 0.6$ and $zT = 1$ with reference value $\alpha_{ref} = 180$ μV/K for $T_{ref} = 300$ K.
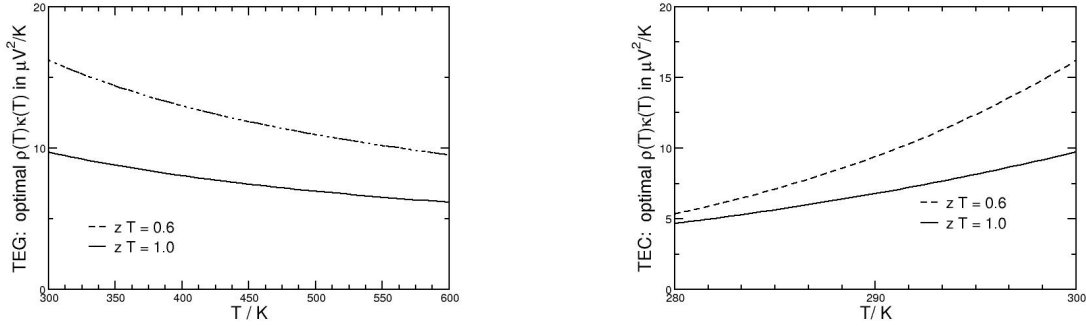

Figure 1.6: Optimal profile for the product $\rho(T)\kappa(T) = T\alpha^2(T)/k_0$ for TEG (left side, $T_a = 600$ K, $T_s = 300$ K); and TEC (right side, $T_a = 280$ K, $T_s = 300$ K) plotted for the constraints $zT = 0.6$ and $zT = 1$ according to the optimal Seebeck profiles shown in Fig. 1.5.

by the integrals (1.39).

Applying Eq. (1.15) for the case of optimal reduced efficiency, we get with the optimal TE potential from Eq. (1.14)

$$\text{TEG:} \quad \eta_{r0} = \frac{T(x)\Phi'(x)}{T'(x)\Phi(x)} = \frac{\alpha'(x)T(x)}{T'(x)\alpha(x)} + 1 \ , \quad \text{TEC:} \quad \frac{1}{\eta_{r0}} = \frac{\alpha'(x)T(x)}{T'(x)\alpha(x)} + 1 \ ,$$

leading to similar differential equations for both TEG and TEC

$$\text{TEG:} \quad \frac{\alpha'(x)}{\alpha(x)} = \ (\eta_{r0} - 1)\frac{T'(x)}{T(x)} \equiv k_g \frac{T'(x)}{T(x)} \tag{1.46a}$$

and

$$\text{TEC:} \quad \frac{\alpha'(x)}{\alpha(x)} = \left(\frac{1}{\eta_{\text{r}0}} - 1 \right) \frac{T'(x)}{T(x)} \equiv k_c \frac{T'(x)}{T(x)} \ . \tag{1.46b}$$

A simple integration gives a correlation between the optimal temperature profile and the optimal, spatial Seebeck coefficient for both TEG and TEC (again with $\alpha_{\text{ref}} = \alpha(T_{\text{ref}})$) which is equivalent to Eqs. (1.45a) and (1.45b):

$$\text{TEG:} \quad \alpha(x) = \alpha_{\text{ref}} \left[\frac{T(x)}{T_{\text{ref}}} \right]^{k_{\text{g}}} , \quad \text{TEC:} \quad \alpha(x) = \alpha_{\text{ref}} \left[\frac{T(x)}{T_{\text{ref}}} \right]^{k_{\text{c}}} . \tag{1.47}$$

Thus, only one material profile must be predefined when using the constraint $z\,T = \text{const}$. In fact Eq. (1.47) represents a third optimization equation within variant B whereas the search for optimal, spatial profiles is then based on only one given profile, e.g. $\kappa(x)$ for maximum η (TEG) and $\sigma(x)$ for maximum φ (TEC), respectively.

1.7 Summary

Fully self-compatible elements are characterized by a set of optimal material profiles whereas optimization is done here within the framework of a 1D model with fixed length of the active material and fixed boundary temperatures. An optimal set of spatial profiles can be found within a thermodynamic optimization procedure together with an optimal temperature profile $T(x)$. However, it has become clear in the last section that all profiles cannot be found simultaneously in a direct way; at least one profile has to be predefined or appropriate constraints established. Nevertheless, there is hope that a combination of thermodynamic optimization based on the appropriate constraints will give a real chance to come closer to the optimal material gradients. For a steady and monotonous optimal temperature profile, the optimal spatial profiles can be transformed into related profiles $\alpha(T)$, $\sigma(T)$ and $\kappa(T)$ in order to compare with real temperature dependent materials data. Alternatively, stacked elements can be used to approach the optimal spatial profiles. However, it would be wrong to reduce FGM research to investigations based on the temperature dependence of given homogeneous or continuously graded materials.

The case of maximum cooling, i. e. determining ΔT_{max} in the TEC case,[17] is obtained when

---

[17]Referring to CPM, we find $T'(L) = 0$ and hence $u(L) \to -\infty$ at the heat-sink side for maximum cooling; this divergence is not found when using optimal gradients.

considering the coefficient of performance in the limit $\varphi \to 0$. It is assumed from the previous section (see Fig. 1.5) that we will get (with a monotonous $T(x)$) a monotonous, optimal Seebeck profile $\alpha(x) = \alpha\,[T(x)]$ also in the case of $\Delta T_{\max}$.

We expect that the use of self-compatible elements is probably the most efficient way to accomplish direct energy conversion in thermoelectrics.

1.8 Outlook and related problems

Further problems concern the electrical power output of a thermogenerator and the heat pumping mode of a Peltier cooler at arbitrary ΔT.

The power output is – unlike η and φ – a purely electrical quantity. For this reason, the integral kernel does not only depend on u but also on j explicitly; from results published in [155, 157] we find the integral for the net electrical power output density

$$p_{\mathrm{net}} = -\frac{P}{A_{\mathrm{c}}} = \int_{T_{\mathrm{s}}}^{T_{\mathrm{a}}} K^P(j, u)\,dT = -\int_{T_{\mathrm{a}}}^{T_{\mathrm{s}}} K^P(j, u)\,dT \tag{1.48}$$

with

$$K^P(j, u) = j\alpha \left(1 - u\frac{\alpha}{z}\right)\ .$$

Within the concept of power-related compatibility [155] the power compatibility factor has been found to be $s^{(P)} = z/(2\alpha) = \alpha\,\sigma/(2\kappa)$. Proof can be given also from Eq. (1.48) if we evaluate the derivation of the kernel K^P with respect to j

$$\frac{\partial K^P}{\partial j} = \alpha \left(1 - u\frac{\alpha}{z}\right) - j\,\alpha\,\frac{\alpha}{z}\frac{\partial u}{\partial j} = \alpha - 2\,u\,\frac{\alpha^2}{z} = 0$$
$$\Longrightarrow\ u_{\mathrm{opt},P} = \frac{z}{2\,\alpha} = s^{(\mathrm{g},P)}\ , \tag{1.49}$$

where $\partial u/\partial j = u/j$ has been used which follows from the definition of u.

The power compatibility factor $s^{(P)}$ has been proved to be the first order approximation of the TEG's efficiency compatibility factor. This means that optimization strategies for power output and η will lead (apart from minor differences) to similar results especially for small $z\,T$ values.

The target of the optimization procedure for the power output of a TEG of fixed length is to find not only the optimum u but also explicitly the optimum electrical current density. Results are published in a separate paper [158], therewith continuing previous investigations on graded thermogenerators [72, 165, 174, 176, 183].

Considering maximum performance parameters P, η and φ for the CPM case (averages), there is a monotonous temperature profile as well as a monotonous $u(x)$ over the length of the TE element ($u > 0$ for TEG, but $u < 0$ for φ of a TEC). The situation changes essentially if Peltier cooler modes close to maximum heat pumping shall be investigated. In this case, we find a changing sign of $T'(x)$ because $T(x)$ peaks in the interior of the TE element. Clearly, based on a suitable integral formulation, this mode could also be treated in an appropriate manner. However, it should be noticed that then "pump up" ($T'(x) > 0$) and "pump down" ($T'(x) < 0$) sections have to be treated separately. It has also to be considered whether (following Sherman's intention)[18] $y = 1/u$ is the more practical variable [160] when performing calculations on TEC. This formulation may also be beneficial when examining maximum heat pumping and the TE heater (TEH), respectively.

---

[18]Sherman used the temperature T as independent variable; thus $y(T) = -\kappa(T)/[j\,x'(T)]$ (see Eq. (40) in the original paper [160]).

Bibliography

[1] Milton Abramowitz and Irene A. Stegun, editors. *Handbook of Mathematical Functions with Formulas, Graphs, and Mathematical Tables.* Dover Publications, Inc., 180 Varick Street, New York, N.Y. 10014, 10 edition, 1972.

[2] E. Altenkirch. Über den Nutzeffekt der Thermosäulen. *Physikalische Zeitschrift*, 10:560–580, 1909.

[3] E. Altenkirch. Elektrothermische Kälteerzeugung und reversible elektrische Heizung. *Physikalische Zeitschrift*, 12:920–924, 1911.

[4] L. Anatychuk. The law of thermoelectric induction and extending the capabilities of its application. *Journal of Electronic Materials*, 39:1869–1874, 2010. 10.1007/s11664-009-0983-0.

[5] L. Anatychuk and R. Kobylyansky. Power properties of the transverse short-circuited thermoelement. *Journal of Electronic Materials*, 39:1704–1707, 2010. 10.1007/s11664-010-1205-5.

[6] L.I. Anatychuk. Original thermoelectric development of physical concepts, materials and related technologies and applications. In *Proceedings of XX International Conference on Thermoelectrics (ICT 2001)*, pages 35 –41, 2001.

[7] L.I. Anatychuk. Current status and some prospects of thermoelectricity. In *Proceedings of the 5th European Conference on Thermoelectrics*, Odessa (Ukraine), September 2007.

[8] L.I. Anatychuk and O.J. Luste. Physical principles of microminiaturization in thermoelectricity. In *Fifteenth International Conference on Thermoelectrics, 1996*, pages 279 – 287, March 1996.

[9] L.I. Anatychuk and O.J. Luste. Thermoelectric eddy currents. Calculation and control methods. In *Proceedings ICT '97. XVI International Conference on Thermoelectrics, 1997*, pages 595 –598, August 1997.

[10] L.I. Anatychuk, O.J. Luste, and L.N. Vikhor. Optimal functions as an effective method for thermoelectric devices design. In *Fifteenth International Conference on Thermoelectrics, 1996*, pages 223 –226, March 1996.

[11] L.I. Anatychuk and L.N. Vikhor. Functionally graded materials and new prospects for thermoelectricity use. In *Proceedings ICT '97. XVI International Conference on Thermoelectrics, 1997*, pages 588 –591, aug. 1997.

[12] L.I. Anatychuk and L.N. Vikhor. Physics and methods of FGTM design. In *Twenty-Second International Conference on Thermoelectrics - ICT 2003*, pages 425 – 428, August 2003.

[13] C.A.B. Ball, W.A. Jesser, and J.R. Maddux. The distributed Peltier effect and its influence on cooling devices. In *Proceedings of the 14th International Conference on Thermoelectrics*, pages 305 – 309, 1995.

Bibliography

[14] I.M. Belov, V.P. Volkov, and O. Manyakin. Optimization of peltier thermocouple using distributed Peltier effect. In *Eighteenth International Conference on Thermoelectrics, 1999.*, pages 316 –318, 1999.

[15] David J. Bergman and Leonid G. Fel. Enhancement of thermoelectric power factor in composite thermoelectrics. *Journal of Applied Physics*, 85(12):8205–8216, 1999.

[16] David J. Bergman and Ohad Levy. Composite thermoelectrics - exact results and calculational methods. In G.A. Slack D.D. Allred, C.B. Vining, editor, *Modern Perspectives On Thermoelectrics and Related Materials*, volume 234, pages 39–45. Pittsburgh, PA, 1991.

[17] D.J. Bergman and L.G. Fel. Enhancement of thermoelectric power factor in composite thermoelectrics. In *Eighteenth International Conference on Thermoelectrics, 1999*, pages 76 –79, 1999.

[18] Zhixi Bian and Ali Shakouri. Beating the maximum cooling limit with graded thermoelectric materials. *Applied Physics Letters*, 89(21):212101, 2006.

[19] Zhixi Bian, Hongyun Wang, Qiaoer Zhou, and Ali Shakouri. Maximum cooling temperature and uniform efficiency criterion for inhomogeneous thermoelectric materials. *Physical Review B (Condensed Matter and Materials Physics)*, 75(24):245208, 2007.

[20] U. Birkholz, E. Groß, M. Riffel, H. Roth, U. Stöhrer, and W. Wittmer. Measurement of the efficiency of a HMS-FeSi$_2$ thermoelectric generator. In *Proc. 11th Int. Conf. on Thermoelectrics*, pages 51–54, Arlington, 1992.

[21] Ulrich Birkholz. Zur experimentellen Bestimmung der thermoelektrischen Effektivität von Halbleitern. *Solid-State Electronics*, 1(1):34 – 38, 1960.

[22] J.M. Borrego. Carrier concentration optimization in semiconductor thermoelements. *IEEE Transactions on Electron Devices*, 10(6):364 – 370, November 1963.

[23] Jose M. Borrego. Approximate analysis of the operation of thermoelectric generators with temperature dependent parameters. *IEEE Transactions on Aerospace*, 2:4–9, 1964.

[24] A. E. Bowley, L. E. J. Cowles, G. J. Williams, and H. J. Goldsmid. Measurement of the figure of merit of a thermoelectric material. *Journal of Scientific Instruments*, 38(11):433, 1961.

[25] Shawna R. Brown, Susan M. Kauzlarich, Franck Gascoin, and G. Jeffrey Snyder. Yb$_{14}$ Mn Sb$_{11}$: new high efficiency thermoelectric material for power generation. *Chemistry of Materials*, 18(7):1873–1877, April 2006.

[26] I. S. Buda and V. S. Lutsyak. The theory of an anisotropic thermoelectric cooler in a magnetic field. *physica status solidi (a)*, 147(2):491–496, 1995.

[27] I. S. Buda, V. S. Lutsyak, U. M. Khamets, and L. A. Shcherbina. Thermodynamic definition of the thermoelectric figure of merit of an anisotropic medium. *physica status solidi (a)*, 123(2):K139–K143, 1991.

[28] Richard J. Buist. The extrinsic Thomson effect. In *Proceedings of the 14th International Conference on Thermoelectrics*, pages 301 – 304, 1995.

[29] Irvin B. Cadoff and Edward Miller. The thermoelectric circuit. In Irvin B. Cadoff and Edward Miller, editors, *Thermoelectric Materials and Devices*, Materials Technology Series, chapter 2, pages 18–32. Reinhold Publishing Cooperation, New York, 1960.

[30] Irvin B. Cadoff and Edward Miller, editors. *Thermoelectric Materials and Devices*, Materials Technology Series, New York, 1960. Reinhold Publishing Cooperation. Lectures presented during the course on Thermoelectric Materials and Devices sponsored by the Department of Metallurgical Engineering in cooperation with the Office of Special Services to Business and Industry, New York, N.Y., June 1959 and 1960.

[31] Herbert B. Callen. *On the theory of irreversible processes*. PhD thesis, M.I.T., 1947.

[32] Herbert B. Callen. The application of Onsager's reciprocal relations to thermoelectric, thermomagnetic, and galvanomagnetic effects. *Phys. Rev.*, 73(11):1349–1358, June 1948.

[33] Herbert B. Callen. *Thermodynamics and an Introduction to Thermostatistics*. John Wiley & Sons, Inc., 2. edition, 1985.

[34] Min Chen, L.A. Rosendahl, T.J. Condra, and J.K. Pedersen. Numerical modeling of thermoelectric generators with varing material properties in a circuit simulator. *Energy Conversion, IEEE Transactions on*, 24(1):112–124, March 2009.

[35] W.H. Clingman. Entropy production and optimum device design. *Advanced Energy Conversion*, 1:61 – 79, 1961.

[36] W.H. Clingman. New concepts in thermoelectric device design. *Proceedings of the IRE*, 49(7):1155 –1160, July 1961.

[37] Milan H. Cobble. Calculations of generator performance. In David Mike Rowe, editor, *CRC Handbook of Thermoelectrics*, chapter 39, pages 489–501. CRC Press, RC, Boca Raton, FL, 1995.

[38] Z. Dashevsky, Y. Gelbstein, I. Edry, I. Drabkin, and M.P. Dariel. Optimization of thermoelectric efficiency in graded materials. In *Proceedings of the 22nd International Conference on Thermoelectrics*, pages 421 – 424, 2003.

[39] Z. Dashevsky, S. Shusterman, M. P. Dariel, and I. Drabkin. Thermoelectric efficiency in graded indium-doped PbTe crystals. *Journal of Applied Physics*, 92(3):1425–1430, 2002.

[40] S. de Groot and P. Mazur. *Non-equilibrium thermodynamics*. Dover, London, 1984 (reprinted).

[41] S. R. de Groot. *Thermodynamics of irreversible processes*. North-Holland Publishing Company, Amstedam, 1963.

[42] K. G. Denbigh. *The thermodynamics of the steady state*. John Wiley & Sons, Inc., New York, 1951.

[43] Charles A. Domenicali. Irreversible thermodynamics of thermoelectric effects in inhomogeneous, anisotropic media. *Phys. Rev.*, 92(4):877–881, November 1953.

[44] Charles A. Domenicali. Irreversible thermodynamics of thermoelectricity. *Rev. Mod. Phys.*, 26(2):237–275, April 1954.

[45] Charles A. Domenicali. Stationary temperature distribution in an electrically heated conductor. *Journal of Applied Physics*, 25(10):1310–1311, 1954.

[46] A.D. Downey and T.P. Hogan. Circuit model of a thermoelectric module for ac electrical measurements. In *24th International Conference on Thermoelectrics, ICT 2005*, pages 79 – 82, June 2005.

Bibliography

[47] Adam D. Downey, Timothy P. Hogan, and Bruce Cook. Characterization of thermoelectric elements and devices by impedance spectroscopy. *Review of Scientific Instruments*, 78(9):093904, 2007.

[48] D. Ebling, K. Bartholomé, M. Bartel, and M. Jägle. Module geometry and contact resistance of thermoelectric generators analyzed by multiphysics simulation. *Journal of Electronic Materials*, 39:1376–1380, 2010. 10.1007/s11664-010-1331-0.

[49] A.A. Efremov and A.S. Pushkars. Energy calculation of thermoelements with arbitrary temperature dependence of thermoelectric properties of materials by heat balance technique. *Energy conversion*, 11(3):101–104, 1971.

[50] Paul H. Egli. *Thermoelectricity*. John Wiley & Sons, Inc., New York, 1960.

[51] M. R. El-Saden. Irreversible thermodynamics and the theoretical bound on the thermomagnetic figure of merit. *Journal of Applied Physics*, 33(10):3145–3146, 1962.

[52] Donald D. Fitts. *Nonequilibrium thermodynamics: A phenomenological theory of irreversible processes in fluid systems*. McGraw-Hill, New York, 1962.

[53] G. Fraisse, M. Lazard, C. Goupil, and J.Y. Serrat. Study of a thermoelement's behaviour through a modelling based on electrical analogy. *International Journal of Heat and Mass Transfer*, 53(17-18):3503 – 3512, 2010.

[54] Steven I. Freedman. Thermoelectric power generation. In George W. Sutton, editor, *Direct Energy Conversion*, volume 3 of *Inter-University Electronic Series*, chapter 3, pages 105–180. McGraw-Hill Book Company, 1966.

[55] Michael Freunek, Monika Müller, Tolgay Ungan, William Walker, and Leonhard M. Reindl. New physical model for thermoelectric generators. *Journal of Electronic Materials*, 38(7):1214–1220, 2009.

[56] Nicholas Fuschillo. Thermoelectric phenomena. In Irvin B. Cadoff and Edward Miller, editors, *Thermoelectric Materials and Devices*, Materials Technology Series, chapter 1, pages 1–17. Reinhold Publishing Cooperation, New York, 1960.

[57] F. Gascoin, C. Goupil, C. de Vaulx, and A. Papavero. Non-homogeneous thermoelectric material study using the linear reponse approach. In *Proceedings of the 29th International Conference on Thermoelectrics*, pages 305 – 309, 2010.

[58] Y. Gelbstein, Z. Dashevsky, and M.P. Dariel. High performance n-type PbTe-based materials for thermoelectric applications. *Physica B: Condensed Matter*, 363(1-4):196 – 205, 2005.

[59] H. J. Goldsmid. A new upper limit to the thermoelectric figure-of-merit. In David Mike Rowe, editor, *CRC Handbook of Thermoelectrics: Macro to Nano*, chapter 10. Taylor and Francis, Boca Raton, FL, 2006.

[60] H. Julian Goldsmid. *Electronic refrigeration*. Pion, London, 1986.

[61] H.J. Goldsmid and J.W. Sharp. The thermal conductivity of inhomogeneous thermoelectric materials. *physica status solidi (b)*, 241(11):2571–2574, 2004.

[62] Christophe Goupil. Thermodynamics of the thermoelectric potential. *J. Appl. Phys.*, 106:104907, 2009.

[63] Christophe Goupil, Wolfgang Seifert, Knud Zabrocki, Eckhard Müller, and G. Jeffrey Snyder. Thermodynamics of thermoelectric phenomena and applications. *Entropy*, 2011. in preparation.

[64] O.S. Gryaznov, B.Ya. Moizhes, and V.A. Nemchinskii. Generalized thermoelectric efficiency. *Soviet Phys.-Techn. Phys.*, 23(8):975–980, August 1978. Translated from Zhurnal tekhnicheskoi fiziki **48**, p. 1720-1728.

[65] T. C. Harman. Special techniques for measurement of thermoelectric properties. *Journal of Applied Physics*, 29(9):1373–1374, 1958.

[66] T. C. Harman. Measurment of Thermoelectric Properties by Using Peltier Heat. In Paul H. Egli, editor, *Thermoelectricity*, chapter 14, pages 235–255. John Wiley & Sons, Inc., New York, 1960.

[67] T. C. Harman, J. H. Cahn, and M. J. Logan. Measurement of thermal conductivity by utilization of the Peltier effect. *Journal of Applied Physics*, 30(9):1351–1359, 1959.

[68] T. C. Harman, P. J. Taylor, M. P. Walsh, and B. E. LaForge. Quantum Dot Super-lattice Thermoelectric Materials and Devices. *Science*, 297(5590):2229–2232, 2002.

[69] Theodore C. Harman. Measurement of pertinent thermoelectric properties. In Irvin B. Cadoff and Edward Miller, editors, *Thermoelectric Materials and Devices*, Materials Technology Series, chapter 6, pages 84–97. Reinhold Publishing Cooperation, New York, 1960.

[70] Theodore Carter Harman and Jürgen M. Honig. *Thermoelectric and thermomagnetic effects and applications*. McGraw-Hill Book Company, New York, 1967.

[71] Robert R. Heikes and Jr. Roland W. Ure. *Thermoelectricity: Science and Engineering*. Interscience Publishers, Inc., New York, 1961.

[72] L. Helmers, Eckhard Müller, J. Schilz, and W.A. Kaysser. Graded and stacked thermoelectric generators - numerical description and maximisation of output power. *Materials Science and Engineering B*, 56(1):60–68, 1998.

[73] Conyers Herring. Effect of random inhomogeneities on electrical and galvanomagnetic measurements. *Journal of Applied Physics*, 31(11):1939–1953, 1960.

[74] Timothy P. Hogan and Tom Shih. Modeling and characterization of power generation modules based on bulk materials. In David Mike Rowe, editor, *CRC Handbook of Thermoelectrics: Macro to Nano*, chapter 12. Taylor and Francis, Boca Raton, FL, 2006.

[75] A.F. Ioffe. *Semiconductor thermoelements and thermoelectric cooling*. London, Infosearch, ltd., 1957.

[76] H. Iwasaki and H. Hori. Thermoelectric property measurements by the improved Harman method. In *24th International Conference on Thermoelectrics, 2005. ICT 2005*, pages 513 – 516, June 2005.

[77] Hideo Iwasaki, Mikio Koyano, and Hidenobu Hori. Evaluation of the figure of merit on thermoelectric materials by Harman method. *Japanese Journal of Applied Physics*, 41(Part 1, No. 11A):6606–6609, 2002.

[78] A. Jacquot, M. Jägle, J. König, D.G. Ebling, and H. Böttner. Theoretical study of the Harman-method for evaluating the thermoelectric performance of materials and components at high temperature. In *Proceedings of the 5th European Conference on Thermoelectrics*, Odessa (Ukraine), September 2007.

[79] Martin Jägle. Simulating thermoelectric effects with finite element analysis using COMSOL. In *Proceedings of the 5th European Conference on Thermoelectrics*, Odessa (Ukraine), September 2007.

[80] A. F. Joffe and L. S. Stil'bans. Physical problems of thermoelectricity. *Reports on Progress in Physics*, 22(1):167, 1959.

[81] V. Jovovic and J. Heremans. Doping effects on the thermoelectric properties of $AgSbTe_2$. *Journal of Electronic Materials*, 38:1504–1509, 2009. 10.1007/s11664-009-0669-7.

[82] A.E. Kaliazin, V.L. Kuznetsov, and D.M. Rowe. Rigorous calculations related to functionally graded and segmented thermoelements. In *Proceedings ICT 2001. XX International Conference on Thermoelectrics, 2001*, pages 286 –292, 2001.

[83] Kozo Katayama and Hiromichi Umemiya. Measurement of thermal properties of semiconductor by utilization of the Peltier effect. *Bulletin of JSME*, 12(50):265–272, 1969.

[84] Douglas L. Kerr. Design calculations for thermoelectric generators. In Irvin B. Cadoff and Edward Miller, editors, *Thermoelectric Materials and Devices*, Materials Technology Series, chapter 16, pages 227–249. Reinhold Publishing Cooperation, New York, 1960.

[85] Scott Kirkpatrick. Percolation and conduction. *Rev. Mod. Phys.*, 45(4):574–588, October 1973.

[86] Philipp H. Klein. Properties affecting the utility of thermoelectric materials. In Irvin B. Cadoff and Edward Miller, editors, *Thermoelectric Materials and Devices*, Materials Technology Series, chapter 5, pages 55–83. Reinhold Publishing Cooperation, New York, 1960.

[87] Philipp H. Klein. The $S - \rho$ Meter: A Device for Rapid Measurement of Seebeck Coefficients and Electrical Resistivities at Temperatures up to 1000 C. In Paul H. Egli, editor, *Thermoelectricity*, chapter 15, pages 256–269. John Wiley & Sons, Inc., New York, 1960.

[88] W. Kobayashi, W. Tamura, and I. Terasaki. Thermal conductivity and dimensionless figure of merit of thermoelectric rhodium oxides measured by a modified Harman method. *Journal of Electronic Materials*, 38:964–967, 2009. 10.1007/s11664-009-0788-1.

[89] M. Korzhuev. Increase in the efficiency of thermoelectric heaters by using inhomogeneous branches. *Technical Physics*, 54:1241–1243, 2009. 10.1134/S106378420908026X.

[90] M. Korzhuev. Symmetry analysis of thermoelectric energy converters with inhomogeneous legs. *Journal of Electronic Materials*, 39:1381–1385, 2010. 10.1007/s11664-010-1330-1.

[91] M. Korzhuev and E. Avilov. Use of the Harman technique for figure of merit measurements of cascade thermoelectric converters. *Journal of Electronic Materials*, 39:1499–1503, 2010. 10.1007/s11664-010-1301-6.

[92] M.A. Korzhuev and I.V. Katin. On the placement of thermoelectric generators in automobiles. *Journal of Electronic Materials*, 39:1390–1394, 2010. 10.1007/s11664-010-1332-z.

[93] M.A. Korzhuev, L.D.Ivanova, L.I. Petrova, Yu.V.Granatkina, and T.E. Svechnikova. The multistage thermoelectric devices with inhomogeneous legs. In *Proceedings of the 5th European Conference on Thermoelectrics*, Odessa (Ukraine), September 2007.

[94] V. L. Kuznetsov. Functionally graded materials for thermoelectric applications. In *CRC Handbook of Thermoelectrics: Macro to Nano*, chapter 38. Taylor and Francis, Boca Raton, FL, December 2006.

[95] V. L. Kuznetsov, L. A. Kuznetsova, A. E. Kaliazin, and D. M. Rowe. High performance functionally graded and segmented Bi_2Te_3-based materials for thermoelectric power generation. *Journal of Materials Science*, 37:2893–2897, 2002. 10.1023/A:1016092224833.

[96] Rolf Landauer. Electrical transport and optical properties of inhomogeneous media. In J. C. Garland and D. B. Tanner, editors, *Proceedings of the First Conference on the Electrical Transport and Optical Properties of Inhomogeneous Media*, volume 40 of *AIP Conf. Proc.*, New York, 1978. Ohio State University.

[97] K. Landecker. Some aspects of the performance of refrigerating thermojunctions with radial flow of current. *Journal of Applied Physics*, 47(5):1846 –1851, May 1976.

[98] K. Landecker. On power-generating thermojunctions with radial flow of current. *Solar Energy*, 19(5):439 – 443, 1977.

[99] K. Landecker. Heat transport in coaxial thermoelectric disks with radial flow of current. *Journal of Applied Physics*, 49(9):4939 –4941, September 1978.

[100] M. Lazard, E. Rapp, and H. Scherrer. Some considerations towards design and optimization of segmented thermoelectric generators. In *Proceedings of the 5th European Conference on Thermoelectrics*, Odessa (Ukraine), September 2007.

[101] Myriam Lazard. Heat transfer in thermoelectricity: Modelling, optimization and design. In *Proceedings of the 7th IASME/WSEAS International conference on heat transfer, thermal engineering and environment*, pages 129–134, 2009.

[102] John H. Lienhard IV and John H. Lienhard V. *A heat transfer textbook*. Phlogiston Press, Cambridge, Massachusetts, USA, 3. edition, 2008.

[103] Howard Littman. A clarification of the theoretical upper bound on the thermoelectric "figure of merit" derived from irreversible thermodynamics. *Journal of Applied Physics*, 33(8):2655–2656, 1962.

[104] Howard Littman and Burton Davidson. Theoretical bound on the thermoelectric figure of merit from irreversible thermodynamics. *Journal of Applied Physics*, 32(2):217–219, 1961.

[105] Antonio López, Francisco Villasevil, G. Noriega, and D. Platzek. Thermoelectric integrated numerical modeling process of a temperature and humidity control device apply to vehicles for fogging preventing. In *Proceedings of the 5th European Conference on Thermoelectrics*, Odessa (Ukraine), September 2007.

[106] D.K.C. MacDonald. *Thermoelectricity: An Introduction to the Principles*. Dover Publications, Inc., New York, 2006.

Bibliography

[107] G. D. Mahan. Inhomogeneous thermoelectrics. *Journal of Applied Physics*, 70(8):4551–4554, 1991.

[108] G. D. Mahan. Density variations in thermoelectrics. *Journal of Applied Physics*, 87(10):7326–7332, 2000.

[109] George Ballard Mathews and Ernst Meissel. *A treatise on Bessel Functions and their Applications to Physics*. BiblioBazaar, LLC, 2008.

[110] G. Min and D. M. Rowe. "Symbiotic" application of thermoelectric conversion for fluid preheating/power generation. *Energy Conversion and Management*, 43(2):221 – 228, 2002.

[111] Gao Min. Thermoelectric module design theories. In David Mike Rowe, editor, *CRC Handbook of Thermoelectrics: Macro to Nano*, chapter 11. Taylor and Francis, Boca Raton, FL, 2006.

[112] Gao Min and D. M. Rowe. Improved model for calculating the coefficient of performance of a Peltier module. *Energy Conversion and Management*, 41(2):163 – 171, 2000.

[113] Gao Min and D M Rowe. Ring-structured thermoelectric module. *Semiconductor Science and Technology*, 22(8):880, 2007.

[114] Gao Min and David Mike Rowe. Peltier devices as generators. In David Mike Rowe, editor, *CRC Handbook of Thermoelectrics*, chapter 38, pages 479–488. CRC Press, RC, Boca Raton, FL, 1995.

[115] Gao Min and D.M. Rowe. Optimisation of thermoelectric module geometry for 'waste heat' electric power generation. *Journal of Power Sources*, 38(3):253 – 259, 1992.

[116] Gao Min, D.M. Rowe, and K. Kontostavlakis. Thermoelectric figure-of-merit under large temperature differences. *Journal of Physics D: Applied Physics*, 37(8):1301–1304, 2004.

[117] Gao Min and . Md Yatim. Variable thermal resistor based on self-powered Peltier effect. *Journal of Physics D: Applied Physics*, 41(22):222001, 2008.

[118] A. J. Minnich, M. S. Dresselhaus, Z. F. Ren, and G. Chen. Bulk nanostructured thermoelectric materials: current research and future prospects. *Energy & Environmental Science*, 2(5):466–479, 2009.

[119] B. Ya. Moizhes. The influence of the temperature dependence of physical parameters on the efficiency of thermoelectric generators and refrigerators. *Soviet Physics - Solid State*, 2:728–737, April 1960. Translated from Fizika Tverdogo Tela.

[120] B.Ya. Moizhes, A.V. Petrov, Yu.P. Shishkin, and L.A. Kolomoets. On the choice of the optimal mode of operation of a cascade thermoelectric element. *Sov. Phys.-Techn. Phys.*, 7:336, 1962.

[121] Alexandru Mihail Morega, Mihaela Morega, and Marius A. Panait. Structural optimization of a thermoelectric generator by numerical simulation. *Revue Roumaine des sciences techniques - Serie Électrotechnique et Énergétique*, 55(1):3–12, 2010.

[122] E. Müller, Č. Drašar, J. Schilz, and W. A. Kaysser. Functionally graded materials for sensor and energy applications. *Materials Science and Engineering A*, 362(1-2):17 – 39, 2003. Papers from the German Priority Programme (Functionally Graded Materials).

44

[123] Eckhard Müller, Gabriele Karpinski, L. Ming Wu, Steven Walczak, and Wolfgang Seifert. Separated effect of 1D thermoelectric material gradients. In Peter Rogl, editor, *25th International Conference on Thermoelectrics*, pages 204 – 209. IEEE, Picataway, 08 2006.

[124] Eckhard Müller, Gabriele Karpinski, L.M. Wu, Steven Walczak, and Wolfgang Seifert. Numerically based design of thermoelectric elements. In Mike Rowe, editor, *4th European Conference on Thermoelectrics*, 2006.

[125] Eckhard Müller, Christian Stiewe, David Mike Rowe, and S. G. K. Williams. Approaches to thermoelectric standardization. In David Mike Rowe, editor, *CRC Handbook of Thermoelectrics: Macro to Nano*, chapter 26. Taylor and Francis, Boca Raton, FL, 2006.

[126] Eckhard Müller, Steven Walczak, and Wolfgang Seifert. Optimization strategies for segmented Peltier coolers. *phys. stat. sol. (a)*, 203(8):2128 – 2141, August 2006.

[127] Eckhard Müller, Steven Walczak, Wolfgang Seifert, Christian Stiewe, and Gabriele Karpinski. Numerical performance estimation of segmented thermoelectric elements. In Terry M. Tritt, editor, *ICT 2005 - 24th Int. Conf. on Thermoelectrics*, pages 352 – 357. Institute of Electrical and Electronics Engineers, Inc., 11 2005.

[128] A. Muto, D. Kraemer, Q. Hao, Z. F. Ren, and G. Chen. Thermoelectric properties and efficiency measurements under large temperature differences. *Review of Scientific Instruments*, 80(9):093901, 2009.

[129] M. H. Norwood. A comparison of theory and experiment for a thermoelectric cooler. *Journal of Applied Physics*, 32(12):2559–2563, 1961.

[130] Lars Onsager. Reciprocal relations in irreversible processes. i. *Phys. Rev.*, 37(4):405–426, Feb 1931.

[131] Lars Onsager. Reciprocal relations in irreversible processes. ii. *Phys. Rev.*, 38(12):2265–2279, Dec 1931.

[132] Lars Onsager. Theories and problems of liquid diffusion. *Annals of the New York Academy of Sciences*, 46:241–265, 1945.

[133] A. W. Penn. The corrections used in the adiabatic measurement of thermal conductivity using the Peltier effect. *Journal of Scientific Instruments*, 41(10):626, 1964.

[134] Noëlle Pottier. *Physique statisitique hors équilibre, processus irréversibles linéaires*. Savoirs Actuels EDP Sciences/CNRS Editions, 2007.

[135] M. Power and R.A. Handelsman. Generalized calculation of thermoelectric efficiency. *Advanced Energy Conversion*, 1:45 – 60, 1961.

[136] Ilya Prigogine. *Introduction to Thermodynamics of Irreversible Processes*. John Wiley & Sons, Inc., New York, 3. edition, July 1968.

[137] L. Rauscher, S. Fujimoto, H. T. Kaibe, and S. Sano. Efficiency determination and general characterization of thermoelectric generators using an absolute measurement of the heat flow. *Measurement Science and Technology*, 16(5):1054, 2005.

[138] L. Rauscher, H.T. Kaibe, H. Ishimabushi, S. Sano, E. Müller, and D. Platzek. New approach for highly accurate efficiency determination of thermoelectric generator modules. In *ICT 2003, Twenty-Second International Conference on Thermoelectrics*, pages 508–511, La Grande-Motte, France, 2003.

Bibliography

[139] A.J. Reddy, E. Siivola, P. Thomas, G. Krueger, and R. Venkatasubramanian. Measurement and analysis of power conversion efficiency in thin-film and segmented thermoelectric devices. In *24th International Conference on Thermoelectrics, ICT 2005*, pages 72 – 75, June 2005.

[140] S. B. Riffat and G. Q. Qiu. Design and characterization of a cylindrical, water-cooled heat sink for thermoelectric air-conditioners. *International Journal of Energy Research*, 30:67–80, 2006.

[141] E. S. Rittner. Comment on "Theoretical bound on the thermoelectric figure of merit from irreversible thermodynamics". *Journal of Applied Physics*, 33(8):2654–2655, 1962.

[142] Yves Rocard. *Thermodynamique.* Masson, Paris, 2. edition, 1967.

[143] F.D. Rosi, B. Abeles, and R.V. Jensen. Materials for thermoelectric refrigeration. *Journal of Physics and Chemistry of Solids*, 10(2-3):191 – 200, 1959.

[144] F.D. Rosi, E.F. Hockings, and N.E. Lindenblad. Semiconducting materials for thermoelectric power generation. *RCA (Radio Cooperation of America) Review*, 22:82–121, 1961.

[145] D. M. Rowe and G. Min. Design theory of thermoelectric modules for electrical power generation. *IEE Proceedings - Science, Measurement and Technology*, 143(6):351–356, 1996.

[146] D. M. Rowe and Gao Min. Evaluation of thermoelectric modules for power generation. *Journal of Power Sources*, 73(2):193 – 198, 1998.

[147] David Mike Rowe, editor. *CRC Handbook of Thermoelectrics.* RC, Boca Raton, FL, 1995.

[148] David Mike Rowe, editor. *CRC Handbook of Thermoelectrics: Macro to Nano.* RC, Boca Raton, FL, 2006.

[149] David Mike Rowe and C.M. Bhandari. *Modern Thermoelectrics.* Reston Publishing Company, Inc., 11480 Sunset Mills Roads, Reston, Virginia 22090, 1983.

[150] A. G. Samoilowitsch and L. L. Korenblit. Gegenwärtiger Stand der Theorie der thermoelektrischen und thermomagnetischen Erscheinungen in Halbleitern. *Fortschritte der Physik*, 1:486– 554, 1953. Unshortened translation of the article published in Uspechi Fiz. Nauk **49**, p. 243 and p.337 (1953).

[151] Emil Sandoz-Rosado and Robert Stevens. Experimental characterization of thermoelectric modules and comparison with theoretical models for power generation. *Journal of Electronic Materials*, 38:1239–1244, 2009. 10.1007/s11664-009-0744-0.

[152] Emil Sandoz-Rosado and Robert Stevens. Robust finite element model for the design of thermoelectric modules. *Journal of Electronic Materials*, 39:1848–1855, 2010. 10.1007/s11664-010-1077-8.

[153] J. Schilz, Eckhard Müller, L. Helmers, Y.S. Kang, Yasutoshi Noda, and Masayuki Niino. On the composition function of graded thermoelectric materials. *Materials Science Forum*, 308-311:647–652, 1999.

[154] W. Seifert, M. Ueltzen, and Eckhard Müller. One-dimensional modelling of thermoelectric cooling. *Physica Status Solidi (a)*, 1(194):277 – 290, 2002.

[155] Wolfgang Seifert, Eckhard Müller, G.Jeffrey Snyder, and Steven Walczak. Compatibility factor for the power output of a thermogenerator. *phys. stat. sol. (RRL)*, 1(6):250–252, 2007.

[156] Wolfgang Seifert, Eckhard Müller, and Steven Walczak. Generalized analytic description of onedimensional non-homogeneous TE cooler and generator elements based on the compatibility approach. In Peter Rogl, editor, *25th International Conference on Thermoelectrics*, pages 714 – 719. IEEE, Picataway, 08 2006.

[157] Wolfgang Seifert, Eckhard Müller, and Steven Walczak. Local optimization strategy based on first principles of thermoelectrics. *phys. stat. sol. (a)*, 205(12):2908–2918, December 2008.

[158] Wolfgang Seifert, Knud Zabrocki, Eckhard Müller, and G.Jeffrey Snyder. Power-related compatibility and maximum electrical power output of a thermogenerator. *phys. stat. sol. (a)*, 207(10):2399–2406, October 2010.

[159] Wolfgang Seifert, Knud Zabrocki, G.Jeffrey Snyder, and Eckhard Müller. The compatibility approach in the classical theory of thermoelectricity seen from the perspective of variational calculus. *phys. stat. sol. (a)*, 207(3):760–765, March 2010.

[160] B. Sherman, R.R. Heikes, and Jr. R.W. Ure. Calculation of efficiency of thermoelectric devices. *J. Appl. Phys.*, 31(1):1 – 16, 1960.

[161] B. Sherman, R.R. Heikes, and R.W. Ure Jr. Calculation of efficiency of thermoelectric devices. In Irvin B. Cadoff and Edward Miller, editors, *Thermoelectric Materials and Devices*, Materials Technology Series, chapter 15, pages 199–226. Reinhold Publishing Cooperation, New York, 1960. Reprint of [160].

[162] I. Shiota and Y. Miyamoto, editors. *Functionally Graded Material 1996*, AIST Tsukuba Research Center, Tsukuba, Japan, October 1996. Proceedings of the 4th international symposium on Functionally Graded Materials, Elsevier.

[163] R.G. Sickert. A thermoelectric refrigerating system for submarines. *Electrical Engineering*, 79(5):364–371, May 1960.

[164] A.A. Snarskii, G.V. Adzhigai, and I.V. Bezsudnov. On the inherent figure of merit of thermoelectric composites. *Journal of Thermoelectricity*, 4:74–81, 2005.

[165] G. Jeffrey Snyder. Application of the compatibility factor to the design of segmented and cascaded thermoelectric generators. *Applied Physics Letters*, 84(13):2436–2438, 2004.

[166] G. Jeffrey Snyder. Thermoelectric power generation: Efficiency and compatibility. In David Mike Rowe, editor, *CRC Handbook of Thermoelectrics: Macro to Nano*, chapter 9. Taylor and Francis, Boca Raton, FL, 2006.

[167] G. Jeffrey Snyder and Eric S. Toberer. Complex thermoelectric materials. *Nature Materials*, 7:105 – 114, 2008.

[168] G. Jeffrey Snyder and Tristan S. Ursell. Thermoelectric efficiency and compatibility. *Phys. Rev. Lett.*, 91(14):148301, October 2003.

[169] G.J. Snyder. Design and optimization of compatible, segmented thermoelectric generators. In *Twenty-Second International Conference on Thermoelectrics - ICT 2003*, pages 443 – 446, August 2003.

Bibliography

[170] Ulrich Stöhrer. Measurement of the transport properties of $FeSi_2$ and HMS by utilization of the Peltier effect in the temperature range 50-800 degrees C. *Measurement Science and Technology*, 5(4):440, 1994.

[171] J.P. Straley. Thermoelectric properties of inhomogeneous materials. *Journal of Physics D: Applied Physics*, 14(11):2101, 1981.

[172] H. Süßmann and E. Müller. Verification of a transport model for p-type $(Bi_{0.5} Sb_{0.5})$ Te_3 and $(Bi_{0.25} Sb_{0.75})$ Te_3 mixed crystals by means of temperature dependent thermoelectric properties below room temperature. In M.V. Vedernikov, M.I. Federov, and A.E. Kaliazin, editors, *Fourteenth International Conference on Thermoelectrics*, pages 1–7, St. Petersburg, Russia, 1995. International Thermoelectric Society.

[173] Jan Tauc. The theory of the thermal EMF of semi-conductors. *Czechoslovak Journal of Physics*, 3:282–302, 1953.

[174] R. Ure and R. Heikes. The figure of merit of a thermoelectric generator. *Advanced Energy Conversion*, 2:177, 1962.

[175] Roland W. Ure, Jr. and Robert R. Heikes. *Theoretical Calculation of Device Performance*, chapter 15, pages 458–517. Interscience Publishers, Inc., New York, 1961.

[176] T.S. Ursell and G.J. Snyder. Compatibility of segmented thermoelectric generators. In *Twenty-First International Conference on Thermoelectrics*, pages 412–417, 2002.

[177] Rama Venkatasubramanian, Edward Siivola, Thomas Colpitts, and Brooks O'Quinn. Thin-film thermoelectric devices with high room-temperature figures of merit. *Nature*, 413:597–602, October 2001.

[178] Cronin B. Vining. The thermoelectric limit $ZT \sim 1$: Fact or artifact. In K.R. Rao, editor, *The XIth International Conference on Thermoelectrics*, Arlington, October 1992. University of Texas.

[179] Cronin B. Vining. The thermoelectric process. In T.M. Tritt, M.G. Kanatzidis, Jr. H.B. Lyon, and G.D. Mahan, editors, *Materials Research Society Symposium Proceedings: Thermoelectric Materials - New Directions and Approaches*, pages 3–13. Mater. Res. Soc., 1997.

[180] Robert H. Vought. Design calculations for Peltier cooling. In Irvin B. Cadoff and Edward Miller, editors, *Thermoelectric Materials and Devices*, Materials Technology Series, chapter 17, pages 250–274. Reinhold Publishing Cooperation, New York, 1960.

[181] Itzhak Webman, Joshua Jortner, and Morrel H. Cohen. Thermoelectric power in inhomogeneous materials. *Phys. Rev. B*, 16(6):2959–2964, Sep 1977.

[182] Lawrence J. Ybarrondo. *Effects of surface heat transfer and spatial property dependence on the optimum performance of a thermoelectric heat pump*. PhD thesis, Georgia Institute of Technology, 1964.

[183] L.J. Ybarrondo and J.Edward Sunderland. Influence of spatially dependent properties on the performance of a thermoelectric heat pump. *Advanced Energy Conversion*, 5(4):383 – 405, 1965.

[184] Wu Yi-Dong, Wang Zhi-Min, and He Yuan-Jin. A new method for calculating the thermoelectric efficiency. *Chinese Physics Letters*, 21(9):1848, 2004.

[185] K. Zabrocki, E. Müller, and W. Seifert. One-dimensional modeling of thermogenerator elements with linear material profiles. *Journal of Electronic Materials*, 39:1724–1729, 2010. 10.1007/s11664-010-1179-3.

[186] K. Zabrocki, E. Müller, W. Seifert, and Steffen Trimper. Performance optimization of a thermoelectric generator element with linear material profiles in a 1D setup, 2011. submitted to Journal of Materials Research.

[187] Knud Zabrocki, Wolfgang Seifert, and Eckhard Müller. Performance optimization of a thermoelectric generator element with linear material profiles in a 1D scheme. In H.L. Tuller, J.D. Baniecki, G.J. Snyder, and J.A. Malen, editors, *Thermoelectric Materials - Growth, Properties, Novel Characterization Methods, and Applications*, volume 1267 of *Mater. Res. Soc. Symp. Proc.*, pages 27–32, Warrendale, PA, 2010.